

1 **The physiological response of the marine platyhelminth *Macrostomum lignano* to**
2 **different environmental oxygen concentrations.**

3 Short title: Response of a flatworm to oxygen variation

4
5 G. A. Rivera-Ingraham*, U. Bickmeyer, D. Abele

6
7 Alfred-Wegener-Institute for Polar and Marine Research.
8 Dept. Functional Ecology
9 Am Handelshafen 12, 27570 Bremerhaven, Germany.

10
11 *Corresponding author: Georgina.Rivera-Ingraham@awi.de / grivera@us.es

12
13
14
15 **ABSTRACT**

16 Respiration rate of meiofauna is difficult to measure, and the response to variations in
17 the environmental oxygen concentrations has so far been mainly addressed through
18 behavioral investigation. We investigated the effect of different oxygen concentrations
19 on the physiology of the marine platyhelminth *Macrostomum lignano*. Respiration was
20 measured using batches of 20 animals in a glass microtiter plate equipped with optical
21 oxygen sensor spots. At higher oxygen saturations (>12kPa), animals showed a clear
22 oxyconforming behavior. However, below this values, the flatworms kept respiration
23 rates constant at $0.064 \pm 0.001 \text{ nmol O}_2 \cdot \text{l}^{-1} \cdot \text{h}^{-1} \cdot \text{ind}^{-1}$ down to 3 kPa $p\text{O}_2$, and this rate was
24 increased in 30% in animals that were reoxygenated after enduring a period of 1.5h in
25 anoxia. Physiological changes related to tissue oxygenation were assessed using live
26 imaging techniques with different fluorophores in animals maintained in normoxic (21
27 kPa), hyperoxic (40 kPa), near anoxic (≈ 0 kPa) conditions and subjected to anoxia-
28 reoxygenation. Ageladine-A and BCECF both indicated that pH_i under near anoxia
29 increases by about 0.07 to 0.10 units. Mitochondrial membrane potential, $\Delta\psi_m$, was
30 higher in anoxic and hyperoxic compared to normoxic conditions (JC1). Staining with
31 ROS sensitive dyes, DHE for detection of superoxide anion ($\text{O}_2^{\bullet-}$) formation and C-
32 H₂DFFDA for other ROS species aside from $\text{O}_2^{\bullet-}$ (H_2O_2 , HOO^{\bullet} and ONOO^{\bullet}), both
33 showed increased ROS formation following anoxia reoxygenation treatment. Animals
34 exposed to hyperoxic, normoxic and anoxic treatments displayed no significant
35 differences in $\text{O}_2^{\bullet-}$ formation, whereas mitochondrial ROS formation as detected by C-
36 H₂DFFDA was higher after hyperoxic exposure and lowest under near anoxia compared
37 to the normoxic control group. *M. lignano* seems to be a species tolerant to a wide range
38 of oxygen concentrations (being able to maintain aerobic metabolism from extremely
39 low $p\text{O}_2$ and up to hyperoxic conditions) which is an essential prerequisite for
40 successfully dealing with the drastic environmental oxygen variations that occur within
41 intertidal sediments.

42
43 **Keywords:** flatworm, live-imaging, meiofauna, respiration.

44
45 Abbreviations used in the text:

46 $\Delta\psi_m$ =mitochondrial membrane potential

47 C-H₂DFFDA= 5-(and-6)-carboxy-2',7'-difluorodihydrofluorescein diacetate

48 DHE=dihydroethidium

49 NH-FSW=Filtered sea water supplemented with 15mM Na-HEPES

- 50 pH_i =intracellular pH
- 51 P_{O_2} =oxygen partial pressure
- 52 ROS=reactive oxygen species
- 53 SDT=sodium diethyl-dithiocarbamate trihydrate
- 54 SOD=superoxide dismutase
- 55

56 INTRODUCTION

57

58 Marine meiofauna colonize the upper sediment layer of the ocean which, especially in
59 coastal and intertidal sediments, can be highly variable with respect to oxygenation. On
60 one hand, wave action and coastal currents often lead to mechanical mixing of oxygen
61 rich surface water into the upper loosely packed sediment layers. Relatively compacted
62 sediment surfaces in shallow waters are often densely colonized by benthic microalgae
63 that cause daily peaks of photosynthetic oxygenation in the upper 1-2 cm of sediment
64 surface. On the other hand, coastal sediments contain high amounts of organic matter
65 from decaying macroalgae or terrestrial and riverine coastal runoff. The chemical and
66 microbial oxygen demand in these sediments is high so that oxygen that diffuses
67 downwards is rapidly consumed. This produces steep sedimentary redox gradients
68 between the upper, sometimes even hyperoxic and the lower suboxic to anoxic layers,
69 which often span no more than 10 to 50 cm below which the sediment becomes
70 chronically anoxic and sulfidic (rich in hydrogen sulfide, H₂S) (Fenchel and Finlay,
71 2008). These sediments are colonized by highly diverse macro- and meiofauna
72 communities, the composition of which varies depending on sediment stability, grain
73 size composition, organic matter content and oxygenation. Whereas macrofauna
74 organisms often build sedimentary burrows that they oxygenate through irrigation with
75 oxygen rich surface waters, meiofauna organisms move between the sand grains,
76 seeking optimal positioning between too high and too low environmental oxygenation
77 according to their metabolic and nutritional requirements. In very few cases, marine
78 meiofauna were shown to actively establish suitable environmental oxygen levels in
79 their closest environment between the sediment grains (Corbari et al., 2005). Much
80 more often it was shown that the meiofauna stratify in response to the sedimentary
81 oxygen gradient (Corbari et al., 2004) and different groups of meiofauna have been
82 described as oxophilic, microoxophilic and thiobiotic according to their preferred
83 positioning in the small scale chemical and redox gradients within the sediment column
84 and around macrofauna burrows (Fenchel and Finlay, 1995; Morrill et al., 1988). This
85 behavior precludes not only that meiofauna species have different metabolic strategies
86 to cope with low and variable environmental oxygenation, but also that they would have
87 means to sense oxygen (and hydrogen sulfide) and react flexibly to changing
88 environmental oxygenation. These reactions include vertical migrations within the
89 sediment column, often away from too high surface oxygenation (Corbari et al., 2005),
90 and/or adjustment of metabolic rate to cope with reduced oxygen availability. However,
91 soft bodied meiofauna worms, such as nematodes and platyhelminths, generally deal
92 with fluctuating tissue oxygenation and changes in environmental redox state because of
93 their small size and fast equilibration time. Whereas several studies have assessed the
94 behavioral (Rosenberg et al., 1991; Tinson and Laybourn-Parry, 1985) and ecological
95 responses to fluctuating oxygenation (Wetzel et al., 2001), studies of the physiological
96 response to fluctuating chemical and oxygenation gradients are scarce.
97 A seminal paper by Morrill et al. (1988) reported antioxidant activities to be better
98 established in thiobiotic than in oxybiotic meiofauna, giving rise to the idea that i)
99 normoxic oxygen levels could already be “hyper-oxic” for these low oxygen adapted
100 species, ii) that the oxidation of toxic H₂S could give rise to the formation of reactive
101 oxygen species (ROS) in thiobiotic, low oxygen adapted meiofauna.
102 In the present study, we investigated the physiological effects of hyperoxic and anoxic
103 exposure conditions in the interstitial marine flatworm *Macrostomum lignano*
104 (Rhabditophora, Macrostomorpha) Ladurner et al, 2005. *M. lignano* has been
105 established as a new model in sexual selection (Schärer et al., 2005) and evolutionary

106 and developmental studies (Egger et al., 2006; Morris et al., 2006), but especially in
107 stem-cell research (Bode et al., 2006; Pfister et al., 2007) and the role of these stem-
108 cells for the process of ageing (Mouton et al., 2009).

109 Platyhelminths are transparent and, thus, elegant model organisms to study cellular and
110 subcellular processes *in vivo*. Using “live imaging” techniques we provide a first set of
111 data regarding the physiological responses of individual flatworms to extreme states of
112 environmental oxygenation and, further, on the effect of anoxia and subsequent
113 reoxygenation on ROS forming processes, mitochondrial membrane potential and tissue
114 pH. We developed a technique to record oxygen partial pressure (pO_2) dependent
115 oxygen consumption rates using batches of 20 flatworms in order to describe their
116 metabolic response to variable environmental oxygenation.

117 In this study we used non-invasive optical techniques to understand how an anoxia
118 tolerant, animal responds to high, low and fluctuating oxygenation, especially with
119 respect to ROS formation, mitochondrial functioning and maintenance pH homeostasis
120 during anoxia-reoxygenation, a detrimental situation in many human pathologies.

121

122 MATERIALS AND METHODS

123 *Animal culturing*

124 Cultures of *M. lignano* (DV-1 line) were reared at the Alfred Wegener Institute
125 (Bremerhaven, Germany) in Petri dishes with Guillard’s F/2 medium at room
126 temperature (RT) (20°C) and fed weekly the diatom *Nitzschia* sp. For experimentation,
127 however, a sterile medium composed of seawater filtered over a 0.2µm Whatman filter
128 and supplemented with 15mM Na-HEPES (NH-FSW) was used. Buffering was
129 necessary to avoid pH changes in the medium when setting anoxic or hyperoxic
130 conditions.

131

132 *Respiration measurements*

133 Two different treatments were considered for the respiration measurements: normoxic
134 (21kPa) and anoxic (0kPa) followed by reoxygenation. For the latter, animals were kept
135 for 1.5h under anoxic conditions (kept in a gas tight glovebox which was equilibrated
136 with 100% N₂ and immersed in an anoxic medium which was prepared by flushing with
137 100% N₂) and later reoxygenated by bubbling with air for an additional 1.5h. Prior to
138 conducting respiration measurements, experimental animals were isolated from the
139 cultures and maintained without food for ca. 20h in NH-FSW. After the acclimation
140 time, 3 groups of 20 animals were transferred with a micropipette to 3 individual wells
141 of a glass microtiter plate (Mikroglas Chemtech GmbH, Mainz, Germany) previously
142 equipped with oxygen sensor spots (SP-PSt3-NAU-D5-YOP, Precision Sensing GmbH,
143 Regensburg, Germany) glued onto the bottom of each well. An additional well was
144 maintained as control, and contained only NH-FSW and the sensor spot. Each of the
145 wells was filled completely with NH-FSW to its maximum capacity which was $100 \pm$
146 $0.5 \mu\text{l}$, to avoid the formation of air bubbles when sealing the wells. Each of the four
147 wells was sealed with a coverslip and the complete surface of the microtiter plate was
148 additionally covered with a layer of auto-adhesive Armaflex[®] (Armacell Enterprise
149 GmbH, Münster, Germany). Additional pressure was maintained on the complete
150 surface of the plate in order to ensure air-tight sealing. Measurements were carried out
151 with a 4-channel fiber-optical oxygen meter (Oxy-4) and non-invasive oxygen sensors
152 (Precision Sensing GmbH, Regensburg, Germany) which were daily calibrated
153 following the manufacturer’s description. Data were recorded at 15sec intervals and the
154 experiments were stopped when the oxygen was completely consumed from each of the
155 animal chambers, which usually took around 16h. All experiments were conducted at

156 RT. Data corresponding to the first 30min following the start of the experiment were
157 discarded in order to avoid interference from stress related to the manipulation of the
158 worms. Respiration rates were expressed as $\text{nmol O}_2 \cdot \text{L}^{-1} \cdot \text{h}^{-1} \cdot \text{ind}^{-1}$. The critical oxygen
159 pressure (p_c) (Tang, 1933) was calculated using the equation of Duggleby (1984).

160

161 *Optical measurements*

162 In this study intracellular pH, mitochondrial membrane potential, mitochondrial density
163 and reactive oxygen species (ROS) concentrations were measured by “live imaging”
164 techniques, which consist in applying specific dyes and *in-vivo* visualization using a
165 Leica TCS SP5II confocal microscope (Leica Microsystems CMS GmbH, Wetzlar,
166 Germany) and a CCD camera system (Visitron Systems GmbH, Puchheim, Germany).

167

168 Four treatments were considered in our study: control (21kPa), anoxia (0kPa),
169 hyperoxia (40kPa) and anoxia followed by reoxygenation. Experiments were carried out
170 in a gas tight glovebox which was equilibrated with either 100% N₂ (anoxia) or 40%
171 O₂/60% N₂ (hyperoxia) using a Wösthoff gas mixing pump (Wösthoff GmbH, Bochum,
172 Germany). Anoxic medium was prepared by flushing with 100% N₂, while hyperoxic
173 NH-FSW medium was obtained by flushing with a 40% O₂-60% N₂ mixture. Thirty
174 minutes flushing were enough for equilibration in all cases as confirmed by
175 measurements of the oxygen content using optical oxygen sensors and the Presens
176 Oximeter (see above).

177 Treatments were conducted with batches of 10 animals which were manipulated at the
178 same time in 2ml Utermöhl chambers for 1.5h. The microscopic chamber in which the
179 animals were anoxically incubated was sealed while still inside of the glovebox and
180 under the gas stream. The chamber was then transferred to the confocal microscope and
181 for the anoxic treatment, it should be noted that we cannot exclude some minor
182 reoxygenation. Thus we decided to use the term of “near anoxia” for the treatment that
183 was aimed to be strict anoxia. After finishing the incubation, a fluorophore was added to
184 the animals in normoxic, anoxic (severely hypoxic) and hyperoxic treatments.

185 For the anoxia-reoxygenation treatment we can assure that the worms were incubated in
186 absolute anoxia, whereupon the chamber was opened and medium and animals were
187 allowed to reoxygenate for an additional 1.5 h. After this time, the dye was added to the
188 reoxygenation treatment. All dyes were used individually for separate batches of
189 animals in order to avoid any possible interference among dyes. The list of the different
190 dyes used in the present study along with their mechanisms of function is given in table
191 1, while incubation and analysis conditions for each of these dyes are detailed in table 2.

192

193 For both of the pH-sensitive dyes used in the present study (ageladine-A and BCECF),
194 further calibration was needed in order to assign numerical pH values to the
195 experimentally recorded intensities/ratios. For ageladine-A (Fujita et al., 2003) this was
196 done following the method described by Bickmeyer et al. (2008) and Bickmeyer (2012)
197 in which the average values obtained for each of the treatments are expressed as a
198 proportion of the control values, and by assuming that non-specialized cells under these
199 control conditions would present a putative pH_i of 7.3-7.4. On the other hand, and since
200 BCECF fluorescence intensity at 490 nm linearly increases between 6.4 and 7.8 pH
201 (Silver, 2003), BCECF results were also converted to pH_i by constructing a calibration
202 curve using the Nigericin technique (Nigericin sodium salt, N7143-5mg, Sigma Aldrich,
203 Germany) described by Thomas et al. (1979).

204 Fluorimetric analysis of the response of the animals to the treatment conditions were
205 carried out in sealed microscope slides using a Leica TCS SP5II confocal microscope.

206 For validation of the pH_i results, further analyses were carried out using a wide-field
207 fluorescence microscope Zeiss Axiovert-10 (Zeiss GmbH, Germany) (equipped a CCD
208 camera system, Visitron, Puchheim, Germany) and applying BCECF staining. For
209 analysis, animals were anesthetized in a 2:1 mixture of 7.14% $MgCl_2 \cdot 6H_2O$ and NH-
210 FSW (Pfannkuche and Thiel, 1988). One picture per individual and per PMT, when
211 ratio calculation was required, was taken for each of the animals using a 10x objective
212 lens. In order to avoid photobleaching, a short period (<5 sec) of low resolution (256 x
213 256 pixel) live scanning was applied for focus adjustments and afterwards only one
214 single scan (512 x 512 pixel) was run of each individual. Autofluorescence was
215 suppressed by adjusting the threshold, and phototoxicity was minimized by the
216 multiphoton laser for low wavelengths scans.

217

218 Image analysis was carried out using Leica LAS Lite software (Leica Microsystems
219 CMS GmbH 2011). Quantification was carried out by plotting 5 transects per animal
220 (always perpendicular to the longitudinal axis of the animal and in all cases selecting the
221 areas of highest intensity, Fig. 1). The maximum value for each transect was obtained
222 and the values of the 5 transects were averaged for each individual.

223

224 Experiments were repeated for a minimum of two times (if results were identical) and
225 up to 12 times, in order to confirm the differences between treatments. Data from the
226 different replicas were pooled. However, since dye uptake by the animals varied among
227 days, the confocal settings needed to be adjusted in order to optimize the quality of the
228 images taken. Thus, data normalization was required prior pooling. Data were
229 normalized by expressing all values within one experimental replica (40 worms) as
230 percentage of the maximum recorded value in that experiment. The maximum value
231 was set to equal 100%. Statistical analyses were performed using SPSS 15.0 (SPSS Inc.,
232 Chicago, IL, USA). Resulting data were compared using ANOVA (followed by
233 Student-Newman-Keuls *a-posteriori* multiple comparison test) when data complied
234 with the assumptions for parametric analyses. When this was not the case, Kruskal-
235 Wallis tests were conducted.

236

237 RESULTS

238 *Respiration measurements*

239 For the normoxic treatment, P_{O_2} dependent respiration rates were analyzed in a total of
240 10 pools, each consisting in 20 animals. Figure 2 shows that respiration rates decreased
241 rapidly (by 70%) between 19 to 12.5kPa in the chamber. Below this po_2 , *M. lignano*
242 starts to regulate respiration down to a low critical po_2 . Thus, for *M. lignano*, a first
243 critical oxygen partial pressure (p_c) was established at 13 kPa (p_{c1}), which marks the
244 point at which the organisms are switching between conformity to regulation. Between
245 12.5 and approximately 3kPa the respiration rates of the worms were constant around
246 $0.064 \pm 0.001 \text{ nmol O}_2 \cdot \text{l}^{-1} \cdot \text{h}^{-1} \cdot \text{ind}^{-1}$. A second p_c appears at $1.36 \pm 0.32 \text{ kPa}$ (p_{c2}), where
247 respiration rates started to decrease again with declining po_2 . Thus, the analysis revealed
248 a high and a low pc above which (p_{c1}) and below which (p_{c2}) the worms switch from
249 regulating to conforming, po_2 dependent respiration. The same pattern was observed for
250 the animals that were previously maintained under anoxic conditions and later
251 reoxygenated. However, the interval at which animals maintained constant respiration
252 rates, values were significantly higher ($0.083 \pm 0.001 \text{ nmol O}_2 \cdot \text{l}^{-1} \cdot \text{h}^{-1} \cdot \text{ind}^{-1}$) ($F=458.23$;
253 $p<0.001$).

254

255 *Activity observations*

256 Normoxic and hyperoxic animals moved rapidly in the Petri dishes with behavioural
257 characteristic best described as unidirectional burst swimming. For microscopic analysis
258 at these high oxygenation levels, the worms had to be anesthetized with $MgCl_2$.
259 Contrary, movement were drastically reduced in anoxia and often the worms started to
260 swim in circles. Many worms were completely immobilized and displayed only
261 epithelial cilia movements. Movements were completely reactivated by reoxygenation,
262 with animals often reaching normoxic levels of activity after 1.5 h under reoxygenated
263 conditions.

264

265 *pH measurements*

266 Staining with the pH sensitive dye ageladine-A (Fig. 3a and supplementary material fig.
267 1a) indicated that the tissue pH levels in anoxic worms or the ones exposed to anoxia-
268 reoxygenation were significantly more alkaline compared to normoxic and hyperoxic
269 animals; ANOVA ($F=10.38$; $p<0.001$). Further estimation of the pH values (using the
270 values of normoxic animals as a reference and assuming that non-specialized cells have
271 a pH of 7.4) indicated a pH-increase by approximately 0.10 units under near anoxia and
272 anoxia-reoxygenation.

273

274 Staining with BCECF (supplementary material fig. 1b) corroborated the general pattern
275 obtained with ageladine in which anoxic and reoxygenated individuals were
276 significantly more basic than the normoxic and hyperoxic treatment groups ($F=3.70$;
277 $p<0.05$) (Fig. 3b). As these results contradicted all our assumptions that animals
278 exposed to near anoxia should become, if anything, more acidic, we applied yet another
279 approach with the wide-field fluorescence imaging microscope and BCECF. Again,
280 animals under near anoxia and anoxia-reoxygenation had the most alkaline values
281 (supplementary material fig. 2) (showing an average increase of 0.07 units) whereas the
282 normoxic and hyperoxic treated worms had a tissue pH of 7.46.

283

284 *Mitochondrial density and membrane potential specific staining*

285 MitoTracker staining indicated most mitochondria to be located in the animals' body
286 wall in epithelial and muscle cells, as well as around the mouth area (Fig. 4).
287 MitoTracker Green FM (supplementary material fig. 3a) stained different treatment
288 groups with different intensities ($K=54.09$; $p<0.000$). Animals kept under hyperoxic
289 conditions (40 kPa) were stained with highest intensity, theoretically suggesting
290 maximum mitochondrial density in hyperoxic worms, followed by individuals under
291 normoxic conditions which displayed less intensive staining (Fig. 5a). Animals kept in
292 anoxia had the lowest staining values with MitoTracker green, and individuals that were
293 subsequently reoxygenated returned to staining intensity recorded in normoxia.

294 To determine whether the significant differences between differently oxygenated groups
295 were associated with oxygenation dependent capacities for dye uptake, a second
296 experiment was performed in which the animals were stained prior to the exposure to
297 the different oxygenation treatments. With this approach we obtained exactly the same
298 group specific pattern as in the first experiment in which the dye was applied following
299 incubation at different oxygen levels. Therefore we used MitoTracker Deep Red 633 in
300 a third approach (supplementary material fig. 3b), which did not produce a clear group-
301 specific pattern. Pooled data from the 4 replicas conducted with MitoTracker Deep Red
302 633, yielded no significant differences among treatments ($K=6.98$; $p=0.072$) (Fig. 5b).
303 High resolution confocal imagery confirmed staining of individual mitochondria in *M.*
304 *lignano* cells (Fig. 6).

305

306 Staining with the dye JC-1 (supplementary material fig. 3c) indicated significant
307 differences in the chemiosmotic H^+ potential ($\Delta\psi_m$) across the mitochondrial inner
308 membrane among treatments ($F=15.14$; $p<0.001$) (Fig. 5c). The smallest potentials were
309 measured in animals exposed to normoxia and in the ones that were reoxygenated after
310 1.5 h of anoxic incubation. Animals exposed in hyperoxic and anoxic media showed
311 significantly more red/green staining, indicating an elevated membrane potential, i.e. a
312 stronger H^+ gradient.

313

314 *Staining for ROS detection*

315 Superoxide anion ($O_2^{\bullet-}$) concentrations were assessed with dihydroethidium (DHE)
316 (supplementary material fig. 4a). DHE staining was similar in animals exposed to
317 anoxic, normoxic and hyperoxic conditions. Animals that were reoxygenated after a
318 period of 1.5h in anoxia had significantly increased DHE staining compared to all other
319 groups ($K=15.77$; $p<0.001$) (Fig. 7a). Formation of other ROS species aside from $O_2^{\bullet-}$
320 (H_2O_2 , $HOO\bullet$ and $ONOO^{\bullet}$) in *M. lignano* cells were assessed using C-H₂DFFDA
321 (supplementary material fig. 4b), which again showed important differences between
322 treatments ($K=80.82$; $p<0.000$). The staining intensity decreased in the order anoxia-
323 reoxygenation = hyperoxia > normoxia > near anoxia (Fig. 7b) indicating ROS
324 formation to decrease between hyperoxia and anoxia as expected.

325

326 *Effects of superoxide dismutase (SOD) and sodium diethyl-dithiocarbamate trihydrate* 327 *(SDT) on ROS staining*

328 To scrutinize for the causes of the high DHE signal in anoxically incubated worms that
329 should theoretically not be able to form $O_2^{\bullet-}$, we applied a SOD solution (Sigma S-2515)
330 and the SOD inhibitor SDT (Sigma D-3506) to anoxic animals stained with DHE (Fig.
331 8a). The first results with neither SOD nor SDT addition again lead to significant DHE
332 staining (above the background signal) in anoxically incubated specimens, although the
333 values were significantly lower than those obtained with normoxic animals. SOD
334 addition to anoxically incubated animals significantly reduced DHE staining, as $O_2^{\bullet-}$
335 radicals were converted to H_2O_2 at higher rates. Contrary, addition of the SOD-inhibitor
336 SDT caused 2-fold higher DHE fluorescence in anoxic compared to normoxically
337 exposed animals, because less $O_2^{\bullet-}$ radicals were converted to H_2O_2 . Around 90% of the
338 animals died under anoxic exposure with addition of SDT. After performing these tests
339 that indirectly confirm the specificity of DHE for $O_2^{\bullet-}$ detection, we assessed the effect
340 of SOD addition on DHE and C-H₂DFFDA staining in an experiment with both dyes
341 (Fig. 8b). Addition of SOD to the medium of anoxically incubated worms once again
342 significantly reduced $O_2^{\bullet-}$ staining in the DHE-stained worms compared to the normoxic
343 control group. Contrary, SOD addition significantly increased C-H₂DFFDA staining,
344 suggesting higher H_2O_2 concentrations in anoxically incubated SOD supplemented
345 animals than in normoxic controls.

346

347 DISCUSSION

348

349 *M. lignano as marine model organism for live imaging of physiological stress*

350 In the present study we used living *M. lignano* individuals for the application of live
351 imaging techniques. The transparency of this organism allowed an adequate and
352 satisfactory measurement of the physiological parameters taken into account. Moreover,
353 its small size also favoured a fast and complete dye uptake making live imaging with
354 the whole animal possible.

355

356 *Po₂ dependent respiration in M. lignano*

357 Respiration measurements in *M. lignano* cannot be conducted with single animals, and
358 instead require batches of 20 specimens maintained in small volumes (90-100 μ l) of
359 liquid. As the respiration rates are extremely low, measurements need to be conducted
360 in small glass or plexiglass chambers without linings made of Teflon, known to be an
361 oxygen binder.

362 Exposing *M. lignano* to decreasing oxygen concentrations during the respiration
363 measurements indicated that the worms maintain constant consumption rates between 3
364 and 12.5kPa. This could be indicating that this is the species' optimum range of
365 respiration and the animals are actually regulating oxygen consumption, most likely by
366 adjusting ciliary beat frequency. Velocity of ciliary pumping movements may determine
367 the water flow over the body surface which, in this species, also represents the
368 respiratory epithelium. We could not quantify ciliary beat frequency in the present study
369 but, however, we did not observe remarkable differences in cilia movements under
370 different oxygen concentrations. Without being able to rule out the hypothesis that
371 animals are actively regulating ventilation through cilia beating, it should also be
372 considered the possibility that such regulation does not exist and that, in fact, results
373 are driven by mitochondria saturation above 3kPa and that the activity of an alternative
374 oxidase could be responsible for the increase in O₂ consumption above 12.5kPa.
375 Regardless the reason, the range of constant respiration characterizes *M. lignano* as
376 aerobic hypoxia tolerant species. Similar *po₂* dependent respiration patterns have been
377 reported for other marine meiofauna such as oligochaetes (Giere et al., 1999) and the
378 authors suggested this to be an important prerequisite for successfully inhabiting
379 intertidal sediments with microscale spatial variations of the oxygen concentration.
380 Animals that were reoxygenated after enduring a 1.5h period under anoxia, showed a
381 30% increase in their respiration rates, probably due to the stress of the procedure.

382

383 *Responses to high oxygen concentrations*

384 $\Delta\psi_m$, and the way the mitochondrial membrane potential is affected by different oxygen
385 concentrations, has mainly been addressed in mammalian cell cultures. For *M. lignano*
386 the JC1 measurements under normoxia and hyperoxia suggest the increase in oxygen
387 consumption not to be due to mitochondrial uncoupling (opening of the mitochondrial
388 membrane transmission pore, MTP), but to a more intensive respiration, respectively
389 electron flow, which causes increased mitochondrial membrane potential ($\Delta\psi_m$) in
390 hyperoxically exposed worms. Contrary mitochondrial uncoupling and reduction of
391 $\Delta\psi_m$ under hyperoxic conditions has been observed in mammalian microvascular cells
392 (Sastre et al., 2000) and pneumocytes (Guthmann et al., 2005) which impressively
393 highlights the difference between oxyconforming flatworms and oxyregulating
394 mammalian cells. We did not observe aggregation of worms under normoxic/hyperoxic
395 conditions indicating collective re-breathing as observed in ostracods when facing too
396 high oxygen levels (Corbari et al., 2005). Indeed, *M. lignano* would warrant more
397 thorough investigations of its migration or aggregation behaviour within oxygenation
398 structured micro-environments (Fenchel and Finlay, 2008). However, we did observe
399 that the locomotory activity of the worms was conspicuously higher in normoxic and
400 hyperoxically manipulated treatments, with no observable difference between both
401 oxygenation states. Thus, as in many other infaunal species (Abele et al 1998),
402 normoxic oxygen levels are already high for these plathyhelminths and their behaviour
403 indicates an attempt to reduce oxygenation in their sedimentary environment. This
404 increased activity is fuelled by the enhanced respiration above 12.5kPa.

405

406 The C-H₂DFFDA measurements further indicate an increase in ROS (H₂O₂, HOO• and
407 ONOO⁻) production compared to normoxic worms, whereas no effect of hyperoxia on
408 O₂^{•-} concentrations was observed in the DHE measurements. A cross-experiment in
409 which we added either SOD or SOD inhibitor STD to the medium confirmed that the
410 DHE signal depends primarily on the amount of O₂^{•-} in the cells. The measurements
411 with ROS sensitive fluorophores therefore indicate that under hyperoxia the worms
412 SOD activity converts excess O₂^{•-} to H₂O₂. This conversion is abolished by the SOD
413 inhibitor STD which killed the animals when they were exposed under hyperoxic
414 conditions and STD. Mitochondrial production of ROS increases linearly with
415 increasing oxygen concentration (Turrens et al., 1982), and hyperoxia has been shown to
416 elicit oxidative stress and antioxidant responses in marine model organisms (Abele et
417 al., 1998; Lushchak and Bagnyukova, 2006). Interestingly, 12.5kPa is also the limit at
418 which mitochondria of the mammalian lung start to release H₂O₂ at a faster rate
419 compared to lower oxygen levels, indicating antioxidant defenses starting to be
420 overwhelmed. It seems a bit far-fetched to suggest a common upper *pc* for such distinct
421 systems as meiofauna species and human lung epithelia, but the comparison illustrates
422 the wide applicability of the hypothesis that in very diverse systems *po*₂ is kept at very
423 low levels to prevent hyperoxic ROS production.

424
425 pH of the tissue in hyperoxia was shown to be slightly more acidic than in animals kept
426 under normoxic conditions. This can result from various mechanisms such as
427 intensified hydrolysis of ATP and oxidative inhibition of the Na/H⁺ antiporter under
428 enhanced oxidative stress, as reported for brain cells (Mulkey et al., 2004) and for
429 crustaceans (Abele-Oeschger et al., 1997). Furthermore, in fish and some crustaceans
430 hyperoxic shocks can result in a reduction of ventilation rates, which cause extracellular
431 acidosis (Gilmour and Perry, 1994; Gilmour, 2001; Wheatly and Toop, 1989).

432 433 *Responses to anoxia and subsequent reoxygenation*

434 Under anoxic conditions *M. lignano* showed drastically reduced movements,
435 presumably an energy saving behaviour in response to the lack of oxygen. A similar
436 response to anoxia has been reported for a wide variety of invertebrate species, like
437 bivalves (e.g. de Zwaan and Wijsman, 1976) or crustaceans (e.g. Hervant et al., 1995).

438
439 Even though we did not obtain numerical $\Delta\psi_m$ results, our data indicate that *M. lignano*
440 mitochondria mount a stronger H⁺ gradient under low oxygen concentrations than at
441 normoxic conditions (Fig. 5). Compared at normoxia, hypoxia tolerant invertebrates
442 have lower $\Delta\psi_m$ values than cold-blooded vertebrate and mammalian mitochondria
443 (Abele et al., 2007; Brookes et al., 1998; Keller et al., 2004). Anoxic *M. lignano* also
444 maintained high $\Delta\psi_m$ values as hyperoxic individuals, reinforcing the view that the
445 species not only tolerates low oxygen concentration but keeps up the mitochondrial
446 proton gradient down to very low *po*₂. Under severely hypoxic to anoxic conditions <
447 1.5 kPa oxygen consumption rates started to decline as oxygen became limiting.
448 Maintenance of the high proton gradient would then be due to reduced energy
449 expenditures including complete absence of swimming mobility so that energetic
450 requirements can be estimated to be minimal. This leads to the conservation of a high
451 H⁺ gradient because of a reduced phosphorylation activity and proton backflow at the
452 ATPase.

453
454 On the other hand, anoxic animals also featured the most alkaline (least acidic)
455 intracellular pH. This is paradoxical in the sense that for many organisms, cells and

456 tissues, severe hypoxia has been demonstrated to lead to a decrease in cellular ATP,
457 increase of the free intracellular calcium concentrations (e.g. Kristián and Siesjö, 1996)
458 and acidification of extra- and intracellular pH (e.g. Bickler, 1992). Only few studies
459 have observed hypoxic alkalization in cancer cells (see review by Webb et al., 2011)
460 and certain mammalian cells and are in keeping with our results (Mitsufuji et al., 1995).
461 Such an alkalization of the intracellular pH during anoxia could well be an adaptive
462 strategy to avoid apoptosis, known to be associated with intracellular acidification
463 (Lagadic-Gossman et al., 2004; Matsuyama et al., 2000). But the question remains how
464 such an increase of pH_i can be achieved. In cancer cells this has been associated with
465 changes in the expression and/or activity of membrane transporters and ion pumps (see
466 Webb et al., 2011). Other authors like Mitsufuji et al. (1995) suggested that the
467 increasing pH values might be attributed to the activation of the Na/H^+ -antiporter during
468 hypoxia. Since the Na^+ gradient across the cellular membrane is maintained by the
469 Na,K -dependent ATP-ase, the driving force for the proton export by the Na/H^+ -
470 antiporter is an energy (ATP) dependent process. The Na/H^+ -antiporter exports
471 intracellular protons, thus increasing pH_i and preventing acidosis until the cellular stores
472 of ATP are exhausted. We have, however, demonstrated that mitochondrial membrane
473 potential and potentially also the electron flow are maintained down to very low oxygen
474 concentrations. Since ATP requirements are reduced through the reduction of
475 locomotion, we assume ATP to be available for the upkeep of the Na^+ gradient and so to
476 stabilize secondary active proton export during severe hypoxia, which would explain
477 less acidic values in our near anoxia exposed worms. Since ATP concentration was not
478 measured in the present study, this hypothesis cannot be corroborated. In future studies
479 ATP concentrations and involvement of membrane transporters in stabilizing
480 intracellular pH can be tested by luminescence assays (ATP+APD) and using specific
481 inhibitors for membrane transporters. Another factor that could theoretically contribute
482 to the more alkaline pH values during periods of low oxygen concentrations would be
483 the decrease in ATP hydrolysis, which also involves H^+ release, due to the reduction of
484 the worms' muscular activity. Although we consider hypoxic alkalisation to be an
485 important new finding based on live imaging techniques and confirmed by usage of two
486 different pH-sensitive dyes, further investigations of this phenomenon are
487 recommended. While no exact calibration in vivo has been yet developed for the use of
488 Ageladine-A, BCECF has a reported accuracy of 0.07 pH units (Franck et al., 1996),
489 which is within the range shift that we have detected in the present study. Further
490 experiments are planned to see whether pH_i alkalisation during hypoxia in the worms
491 is accompanied by an extracellular acidification as observed in cancer cells (Webb et
492 al., 2011).

493
494 The tenet that mitochondrial ROS formation increases linearly with oxygen
495 concentration in cells (Turrens et al., 1982) is also disputable for the worms. Whereas
496 the H_2O_2 formation was in agreement with this theory, $\text{O}_2\bullet^-$ formation follows a
497 different pattern: *M. lignano* individuals under near anoxia showed similar $\text{O}_2\bullet^-$
498 concentrations as normoxic and hyperoxic animals. Under conditions of strict anoxia
499 and thus in the absence of oxygen, ROS can definitely not be produced. In consequence,
500 under so-called anoxia, minimal traces of oxygen must still have been present, enough
501 to cause some $\text{O}_2\bullet^-$ formation in the worms. It is still under debate if ROS can be
502 produced under hypoxia (Hermes-Lima et al., 1998; Hermes-Lima and Zenteno-Savin,
503 2002) and some evidence of this happening first came from direct ROS measurements
504 (Vanden Hoek et al., 1997), followed by detection through resulting DNA damage
505 (Englander et al., 1999). These results can, however, also be explained by the low K_m

506 for O₂ of mitochondrial nitric oxide synthase, which would lead to production of NO,
507 estimated to be around 5-10% of the normal steady rate of NO production (Alvarez et
508 al., 2003). This NO may bind to and inhibit cytochrome oxidase, causing an increase of
509 its K_m for oxygen and, consequently, increased reduction of the upstream electrons
510 transporters such as complex I and III and in consequence, enhance formation of O₂•⁻
511 under hypoxic conditions (reviewed by Turrens, 2003). Further, NO can react with
512 superoxide to form toxic peroxynitrite which can lead to all sorts of macromolecular
513 damage, including DNA damage, and presumably also induce antioxidant systems.
514 Based on the results obtained through the use of SOD and STD and their effect on
515 anoxic individuals, we suggest that SOD might be inhibited during anoxia, which would
516 additionally contribute to the high O₂•⁻ and the low H₂O₂ concentrations recorded under
517 these conditions. For other invertebrate species such as clams, a decrease in SOD
518 expression and activity has also been observed (Monari et al., 2005).

519 *Effect of oxygenation on MitoTracker fluorescence*

520 Mitochondria in *M. lignano* are mainly concentrated in muscular and epithelial cells,
521 providing energy to the numerous cilia and for body contraction. Although both
522 MitoTracker dyes stained the same location, MitoTracker Green FM and MitoTracker
523 Deep Red 633 gave significantly different results (Fig. 5 and supplementary material
524 fig. 3) with respect to the comparison across treatments. Only with MitoTracker Green
525 we observed a decrease in staining under anoxia, which suggests fluorescence of this
526 dye to be negatively affected by anoxic exposure, even though it has been reported to be
527 independent of membrane potential (Métivier et al., 1998). Some studies have
528 demonstrated that this may not be true (Keij et al., 2000), and similar oxygenation
529 dependent patterns of JC-1 and MitoTracker Green FM in *M. lignano* strongly suggest
530 that MitoTracker Green is indeed sensitive to Δψ_m. In that case, MitoTracker Green FM
531 cannot be considered as a useful probe for mitochondrial density in experiments
532 involving variable tissue oxygenation. This is further supported by the fact that
533 MitoTracker Deep Red 633 staining was independent of the experimental oxygenation
534 state and can thus be considered a better tool for determining mitochondrial mass
535 (Haugland, 2002) in this kind of experiment.

536 537 538 539 CONCLUSIONS

540 In an attempt to establish the platyhelminth *M. lignano* as an applicable whole animal
541 model for physiological investigations, we determined its peculiar physiological
542 response to anoxic and hyperoxic exposure at different levels of cellular functioning.
543 The worms are hypoxia tolerant and maintain the mitochondrial proton gradient and
544 presumably also ATP levels during at least two hours of anoxic exposure.
545 Oxyconforming respiration below 3 kPa apparently satisfies the worm's maintenance
546 metabolism and prevents onset of cellular acidosis, while mobility ceases altogether and
547 only ciliary movements are observable in anoxia and severe hypoxia. Elevated DHE
548 fluorescence indicated superoxide formation in near anoxia which might be attributable
549 to diminishment of SOD activity at low tissue oxygenation. However, we suggest that
550 *M. lignano* could also be an interesting model to study hypothetical respiratory chain
551 superoxide formation at low tissue oxygenation under the possible influence of hypoxic
552 NO formation. The response to hyperoxia also differed from mammalian systems, but
553 aligned with other marine invertebrate infauna that increase respiration rates in a pO₂
554 dependent manner above an upper critical p_{c2}. This is often interpreted as an attempt to
555 reduce excess oxygen in the animals' environment and could be characteristic of

556 species that have successfully adapted to deal with the vagaries of environmental
557 oxygenation in intertidal sediments.

558

559

560 ACKNOWLEDGEMENTS

561 The authors would like to thank Nelly Tremblay for her advice and comments on the
562 respiration measurements and further data analysis, Stefanie Meyer for her valuable
563 laboratory assistance and Peter Karuso, Achim Grube and Matthias Köck for kindly
564 supplying the Ageladine-A used in the present study. Thanks also go to Dr. V.
565 Lushchak and one anonymous referee for the comments on the original manuscript.

566

567 FUNDING

568 This study was supported by Fundación Ramón Areces through a post-doctoral grant
569 awarded to G.A.

570

571

572 REFERENCES

573

574 **Abele-Oeschger, D., Sartoris, F. J. and Pörtner, H.-O.** (1997). Hydrogen
575 Peroxide Causes a Decrease in Aerobic Metabolic Rate and in Intracellular pH in the
576 Shrimp *Crangon crangon*. *Comparative Biochemistry and Physiology Part C:*
577 *Pharmacology, Toxicology and Endocrinology* **117**, 123-129.

578 **Abele, D., Großpietsch, H. and Pörtner, H. O.** (1998). Temporal fluctuations
579 and spatial gradients of environmental Po₂, temperature, H₂O₂ and H₂S in its intertidal
580 habitat trigger enzymatic antioxidant protection in the capitellid worm *Heteromastus*
581 *filiformis*. *Marine Ecology Progress Series* **163**, 179-191.

582 **Abele, D., Philipp, E., Gonzalez, P. and Puntarulo, S.** (2007). Marine
583 invertebrate mitochondria and oxidative stress. *Frontiers in Biochemistry* **12**, 933-946.

584 **Alvarez, S., Valdez, L. B., Zaobornyj, T. and Boveris, A.** (2003). Oxygen
585 dependence of mitochondrial nitric oxide synthase activity. *Biochemical and*
586 *Biophysical Research Communications* **305**, 771-775.

587 **Bickler, P. E.** (1992). Cerebral anoxia tolerance in turtles: regulation of
588 intracellular calcium and pH. *American Journal of Physiology - Regulatory, Integrative*
589 *and Comparative Physiology* **263**, R1298-R1302.

590 **Bickmeyer, U.** (2012). The Alkaloid Ageladine A, Originally Isolated from
591 Marine Sponges, Used for pH-Sensitive Imaging of Transparent Marine Animals.
592 *Marine Drugs* **10**, 223-233.

593 **Bickmeyer, U., Grube, A., Klings, K.-W. and Köck, M.** (2008). Ageladine A,
594 a pyrrole-imidazole alkaloid from marine sponges, is a pH sensitive membrane
595 permeable dye. *Biochemical and Biophysical Research Communications* **373**, 419-422.

596 **Bode, A., Salvenmoser, W., Nimeth, K., Mahlke, M., Adamski, Z.,**
597 **Rieger, R., Peter, R. and Ladurner, P.** (2006). Immunogold-labeled S-phase
598 neoblasts, total neoblast number, their distribution, and evidence for arrested neoblasts
599 in *Macrostomum lignano* (Platyhelminthes, Rhabditophora). *Cell and Tissue Research*
600 **325**, 577-587.

601 **Brookes, P. S., Buckingham, J. A., Tenreiro, A. M., Hulbert, A. J. and**
602 **Brand, M. D.** (1998). The Proton Permeability of the Inner Membrane of Liver
603 Mitochondria from Ectothermic and Endothermic Vertebrates and from Obese Rats:
604 Correlations with Standard Metabolic Rate and Phospholipid Fatty Acid Composition.

605 *Comparative Biochemistry and Physiology Part B: Biochemistry and Molecular*
606 *Biology* **119**, 325-334.

607 **Corbari, L., Carbonel, P. and Massabuau, J.-C.** (2005). The early life history
608 of tissue oxygenation in crustaceans: the strategy of the myodocopid ostracod
609 *Cylindroleberis mariae*. *Journal of Experimental Biology* **208**, 661-670.

610 **Corbari, L., Carbonel, P. and Massabuau, J. C.** (2004). How a low tissue O₂
611 strategy could be conserved in early crustaceans? the example of the podocopid
612 ostracods. *Journal of Experimental Biology* **207**, 4415-4425.

613 **de Zwaan, A. and Wijsman, T. C. M.** (1976). Anaerobic metabolism in
614 bivalvia (Mollusca) Characteristics of anaerobic metabolism. *Comparative*
615 *Biochemistry and Physiology Part B: Comparative Biochemistry* **54**, 313-323.

616 **Duggleby, R. G.** (1984). Regression analysis of nonlinear Arrhenius plots: An
617 empirical model and a computer program. *Computers in Biology and Medicine* **14**, 447-
618 455.

619 **Egger, B., Ladurner, P., Nimeth, K., Gschwentner, R. and Rieger, R.** (2006).
620 The regeneration capacity of the flatworm &i&t;Macrostomum lignano —on
621 repeated regeneration, rejuvenation, and the minimal size needed for regeneration.
622 *Development Genes and Evolution* **216**, 565-577.

623 **Englander, E. W., Greeley, G. H., Wang, G., Perez-Polo, J. R. and Lee, H.-**
624 **M.** (1999). Hypoxia-induced mitochondrial and nuclear DNA damage in the rat brain.
625 *Journal of Neuroscience Research* **58**, 262-269.

626 **Fenchel, T. and Finlay, B.** (1995). Ecology and evolution in anoxic worlds.
627 Oxford: Oxford University Press.

628 **Fenchel, T. and Finlay, B.** (2008). Oxygen and the Spatial Structure of
629 Microbial Communities. *Biological Reviews* **83**, 553-569.

630 **Franck, P., Petitpain, N., Cherlet, M., Dardennes, M., Maachi, F., Schutz,**
631 **B., Poisson, L. and Nabet, P.** (1996). Measurement of intracellular pH in cultured cells
632 by flow cytometry with BCECF-AM. *Journal of Biotechnology* **46**, 187-195.

633 **Fujita, M., Nakao, Y., Matsunaga, S., Seiki, M., Itoh, Y., Yamashita, J., van**
634 **Soest, R. W. M. and Fusetani, N.** (2003). Ageladine A: An Antiangiogenic
635 Matrixmetalloproteinase Inhibitor from the Marine Sponge *Agelas nakamurai*1. *Journal*
636 *of the American Chemical Society* **125**, 15700-15701.

637 **Giere, O., Preusse, J. H. and Dubilier, N.** (1999). *Tubificoides benedii*
638 (Tubificidae, Oligochaeta) – a pioneer in hypoxic and sulfidic environments. An
639 overview of adaptive pathways. *Hydrobiologia* **406**, 235-241.

640 **Gilmour, K. and Perry, S.** (1994). The effects of hypoxia, hyperoxia or
641 hypercapnia on the acid-base disequilibrium in the arterial blood of rainbow trout.
642 *Journal of Experimental Biology* **192**, 269-84.

643 **Gilmour, K. M.** (2001). The CO₂/pH ventilatory drive in fish. *Comparative*
644 *Biochemistry and Physiology - Part A: Molecular & Integrative Physiology* **130**, 219-
645 240.

646 **Guthmann, F., Wissel, H., Schachtrup, C., Tölle, A., Rüdiger, M., Spener, F.**
647 **and Rüstow, B.** (2005). Inhibition of TNF α in vivo prevents hyperoxia-mediated
648 activation of caspase 3 in type II cells. *Respiratory Research* **6**, 1465-1475.

649 **Haugland, R. P.** (2002). Handbook of fluorescent probes and research products.
650 USA: Molecular Probes Inc.

651 **Hermes-Lima, M., Storey, J. M. and Storey, K. B.** (1998). Antioxidant
652 defenses and metabolic depression. The hypothesis of preparation for oxidative stress in
653 land snails. *Comp Biochem Phys* **120**, 437-48.

654 **Hermes-Lima, M. and Zenteno-Savin, T.** (2002). Animal response to drastic
655 changes in oxygen availability and physiological oxidative stress. *Comp Biochem Phys*
656 **133C**, 537-556.

657 **Hervant, F., Mathieu, J., Garin, D. and Fréminet, A.** (1995). Behavioral,
658 ventilatory, and metabolic responses to severe hypoxia and subsequent recovery of the
659 hypogean *Niphargus rhenorhodanensis* and the epigean *Gammarus fossarum*
660 (Crustacea: Amphipoda). *Physiological Zoology* **68**, 223-244.

661 **Keij, J. F., Bell-Prince, C. and Steinkamp, J. A.** (2000). Staining of
662 mitochondrial membranes with 10-nonyl acridine orange MitoFluor Green, and
663 MitoTracker Green is affected by mitochondrial membrane potential altering drugs.
664 *Cytometry* **39**, 203-210.

665 **Keller, M., Sommer, A. M., Pörtner, H. O. and Abele, D.** (2004). Seasonality
666 of energetic functioning and production of reactive oxygen species by lugworm
667 (*Arenicola marina*) mitochondria exposed to acute temperature changes. *Journal of*
668 *Experimental Biology* **207**, 2529-38.

669 **Kristián, T. and Siesjö, B. K.** (1996). Calcium-related damage in ischemia. *Life*
670 *Sciences* **59**, 357-367.

671 **Lagadic-Gossman, D., Huc, L. and Lecureur, V.** (2004). Alterations of
672 intracellular pH homeostasis in apoptosis: origins and roles. *Cell death and*
673 *differentiation* **11**, 953-961.

674 **Lushchak, V. I. and Bagnyukova, T. V.** (2006). Effects of different
675 environmental oxygen levels on free radical processes in fish. *Comp Biochem Physiol B*
676 *Biochem Mol Biol*.

677 **Matsuyama, S., Llopis, J., Deveraux, Q. L., Tsien, R. Y. and Reed, J. C.**
678 (2000). Changes in intramitochondrial and cytosolic pH: early events that modulate
679 caspase activation during apoptosis. *Nature cell biology* **2**, 318-325.

680 **Métivier, D., Dallaporta, B., Zamzami, N., Larochette, N., Susin, S. A.,**
681 **Marzo, I. and Kroemer, G.** (1998). Cytofluorometric detection of mitochondrial
682 alterations in early CD95/Fas/APO-1-triggered apoptosis of Jurkat T lymphoma cells.
683 Comparison of seven mitochondrion-specific fluorochromes. *Immunology Letters* **61**,
684 157-163.

685 **Mitsufuji, N., Yoshioka, H., Tominaga, M., Okano, S., Nishiki, T. and**
686 **Sawada, T.** (1995). Intracellular alkalosis during hypoxia in newborn mouse brain in
687 the presence of systemic acidosis: a phosphorus magnetic resonance spectroscopic
688 study. *Brain and Development* **17**, 256-260.

689 **Monari, M., Matozzo, V., Foschi, J., Marin, M. G. and Cattani, O.** (2005).
690 Exposure to anoxia of the clam, *Chamelea gallina*: II: Modulation of superoxide
691 dismutase activity and expression in haemocytes. *Journal of Experimental Marine*
692 *Biology and Ecology* **325**, 175.

693 **Morrill, A. C., Powell, E. N., Bidigare, R. R. and Shick, J. M.** (1988).
694 Adaptations to life in the sulfide system: a comparison of oxygen detoxifying enzymes
695 in thiobiotic and oxybiotic meiofauna (and freshwater planarians). *Journal of*
696 *Comparative Physiology B: Biochemical, Systemic, and Environmental Physiology* **158**,
697 335-344.

698 **Morris, J., Ladurner, P., Rieger, R., Pfister, D., Del Mar De Miguel-Bonet,**
699 **M., Jacobs, D. and Hartenstein, V.** (2006). The *Macrostomum lignano* EST database
700 as a molecular resource for studying platyhelminth development and phylogeny.
701 *Development Genes and Evolution* **216**, 695-707.

702 **Mouton, S., Willems, M., Braeckman, B. P., Egger, B., Ladurner, P.,**
703 **Schärer, L. and Borgonie, G.** (2009). The free-living flatworm *Macrostomum lignano*:
704 A new model organism for ageing research. *Experimental Gerontology* **44**, 243-249.

705 **Mulkey, D. K., Stornetta, R. L., Weston, M. C., Simmons, J. R., Parker, A.,**
706 **Bayliss, D. A. and Guyenet, P. G.** (2004). Respiratory control by ventral surface
707 chemoreceptor neurons in rats. *Nat Neurosci* **7**, 1360-1369.

708 **Pfannkuche, O. and Thiel, H.** (1988). Sample processing. In *Introduction to*
709 *the study of meiofauna*, eds. R. P. Higgins and H. Thiel), pp. 134-145. Washington:
710 Smithsonian Institution.

711 **Pfister, D., De Mulder, K., Phillip, I., Kuales, G., Hrouda, M., Eichberger,**
712 **P., Borgonie, G., Hartenstein, V. and Ladurner, P.** (2007). The exceptional stem cell
713 system of *Macrostomum lignano*: screening for gene expression and studying cell
714 proliferation by hydroxyurea treatment and irradiation. *Frontiers in Zoology* **4**.

715 **Rosenberg, R., Hellman, B. and Johansson, B.** (1991). Hypoxic tolerance of
716 marine benthic fauna. *Marine Ecology Progress Series* **79**, 127-131.

717 **Sastre, J., Pallardo, F. V. and Vina, J.** (2000). Mitochondrial oxidative stress
718 plays a key role in aging and apoptosis. *IUBMB Life* **49**, 427-435.

719 **Schärer, L., Sandner, P. and Michiels, N. K.** (2005). Trade-off between male
720 and female allocation in the simultaneously hermaphroditic flatworm *Macrostomum* sp.
721 *Journal of Evolutionary Biology* **18**, 396-404.

722 **Silver, R. B.** (2003). Ratio Imaging: Measuring Intracellular Ca⁺⁺ and pH in
723 Living Cells. In *Methods in Cell Biology*, vol. Volume 72 eds. W. Leslie and M. Paul),
724 pp. 369-387: Academic Press.

725 **Tang, P.-S.** (1933). On the Rate of Oxygen Consumption by Tissues and Lower
726 Organisms as a Function of Oxygen Tension. *The Quarterly Review of Biology* **8**, 260-
727 274.

728 **Thomas, J. A., Buchsbaum, R. N., Zimniak, A. and Racker, E.** (1979).
729 Intracellular pH measurements in Ehrlich ascites tumor cells utilizing spectroscopic
730 probes generated in situ. *Biochemistry* **18**, 2210-2218.

731 **Tinson, S. and Laybourn-Parry, J.** (1985). The behavioural responses and
732 tolerance of freshwater benthic cyclopoid copepods to hypoxia and anoxia.
733 *Hydrobiologia* **127**, 257-263.

734 **Turrens, J. F.** (2003). Mitochondrial formation of reactive oxygen species. *The*
735 *Journal of Physiology* **552**, 335-344.

736 **Turrens, J. F., Freeman, B. A., Levitt, J. G. and Crapo, J. D.** (1982). The
737 effect of hyperoxia on superoxide production by lung submitochondrial particles.
738 *Archives of Biochemistry and Biophysics* **217**, 401-410.

739 **Vanden Hoek, T. L., Li, C., Shao, Z., Schumacker, P. T. and Becker, L. B.**
740 (1997). Significant Levels of Oxidants are Generated by Isolated Cardiomyocytes
741 During Ischemia Prior to Reperfusion. *Journal of Molecular and Cellular Cardiology*
742 **29**, 2571-2583.

743 **Webb, B. A., Chimenti, M., Jacobson, M. P. and Barber, D. L.** (2011).
744 Dysregulated pH: a perfect storm for cancer progression. *Nature Reviews: Cancer* **11**,
745 671-677.

746 **Wetzel, M. A., Fleeger, J. W. and Powers, S. P.** (2001). Effects of hypoxia and
747 anoxia on meiofauna: a review with new data from the Gulf of Mexico. *Coastal and*
748 *Estuarine Studies* **58**, 165-184.

749 **Wheatly, M. G. and Toop, T.** (1989). Physiological responses of the crayfish
750 *Pacifastacus leniusculus* to environmental hyperoxia: II. Role of the antennal gland in
751 acid-base and ion regulation. *Journal of Experimental Biology* **143**, 53-70.

752
753

754 FIGURE CAPTIONS

755

756 Fig. 1: Quantification process of the resulting confocal images: a total of 5 transects
757 were used for each of the animals under study. These were always perpendicular to the
758 longitudinal axis of the animal and were located on the areas with the highest
759 fluorescence intensities. A. Animal stained with MitoTracker Deep Red 633. B.
760 Transmission image of the same individual.

761

762 Fig. 2: Oxygen consumption rates of *Macrostomum lignano* at different environmental
763 oxygen partial pressures (kPa). Values are pooled in 1% intervals. Black dots represent
764 mean oxygen consumption rates for the 10 replicas conducted, while grey diamonds
765 represent the values obtained for animals that were, after reaching anoxia, further
766 reoxygenated. Whiskers represent the s.e.m. p_{c1} = upper critical oxygen partial pressure;
767 p_{c2} = low critical oxygen partial pressure

768

769 Fig. 3: Bar diagrams showing the quantitative results obtained for the pH measurements
770 through A) Ageladine-A staining and B) BCECF staining (obtained with the confocal
771 microscope). Subfigures 1 (A1 and B1) show the results corresponding to one
772 individual replica of the experiment. Since for each case the pattern was consistent
773 throughout the replicas, data was normalized and pooled (refer to materials and methods
774 section for more details). The corresponding results are shown in subfigures 2 (A2 and
775 B2). Whiskers represent the s.e.m. N=number of replicas conducted.

776

777

778 Fig. 4: Staining of *M. lignano* with MitoTracker Deep Red 633. A) Transmission image
779 of *M. lignano*. B) MitoTracker Deep Red 633 fluorescence of the same individual and
780 showing how the highest mitochondrial densities can be found in the animals' body
781 wall, in epithelial and muscle cells. C) View of the head showing how high
782 mitochondrial density is also registered around the mouth (white arrow).

783

784

785 Fig. 5: Bar diagrams showing the quantitative results obtained for the mitochondrial
786 measurements through A) MitoTracker Green FM and B) MitoTracker Deep Red 633
787 staining for the assessment of mitochondrial density and C) JC-1 staining for the
788 determination of mitochondrial membrane potential ($\Delta\psi_m$). Subfigures 1 (A1, B1, C1)
789 show the results corresponding to one individual replica of the experiment. Since for
790 each case the pattern was consistent throughout the replicas (except for MitoTracker
791 Deep Red 633), data was normalized and pooled (refer to materials and methods section
792 for more details). The corresponding results are shown in subfigures 2 (A2, B2, C2).
793 Whiskers represent the s.e.m. N=number of replicas conducted.

794

795 Fig. 6: High resolution fluorescence images of individual cells of *M. lignano* stained
796 with MitoTracker Green FM under anoxic (A) and normoxic (B) conditions. Confocal
797 imagery. Scale bar=15 μ m.

798

799

800 Fig. 7: Bar diagrams showing the quantitative results obtained in the ROS quantification
801 through A) DHE and B) C-H₂DFFDA staining. Subfigures 1 (A1, B1) show the results
802 corresponding to one individual replica of the experiment. Since for each case the
803 pattern was consistent throughout the replicas, data was normalized and pooled (refer to

804 materials and methods section for more details). The corresponding results are shown in
805 subfigures 2 (A2, B2). Whiskers represent the s.e.m. N=number of replicas conducted.

806

807 Fig. 8: Results on the effect of the inhibition of SOD under anoxic conditions: (a) effect
808 of SOD and SDT on anoxic animals. Groups associated with the same letter (a-b-c-d)
809 belong to the same subset based on a *a-posteriori* multiple comparison test Student-
810 Newman-Keuls (S.N.K.) ($K=27.41$; $p<0.001$); (b) effect of SOD on the concentrations
811 of O_2^- (DHE values) (b1) and H_2O_2 (C-H₂DFFDA values) (b2) in anoxic animals.
812 Whiskers represent the s.e.m. *** $p<0.001$.

813

814

815 SUPPLEMENTARY MATERIAL CAPTIONS

816

817 Fig. 1: Representative fluorescence images obtained during the pH measurements under
818 the confocal microscope for each of the treatments considered. A) Ageladine-A
819 staining. B) BCECF staining.

820

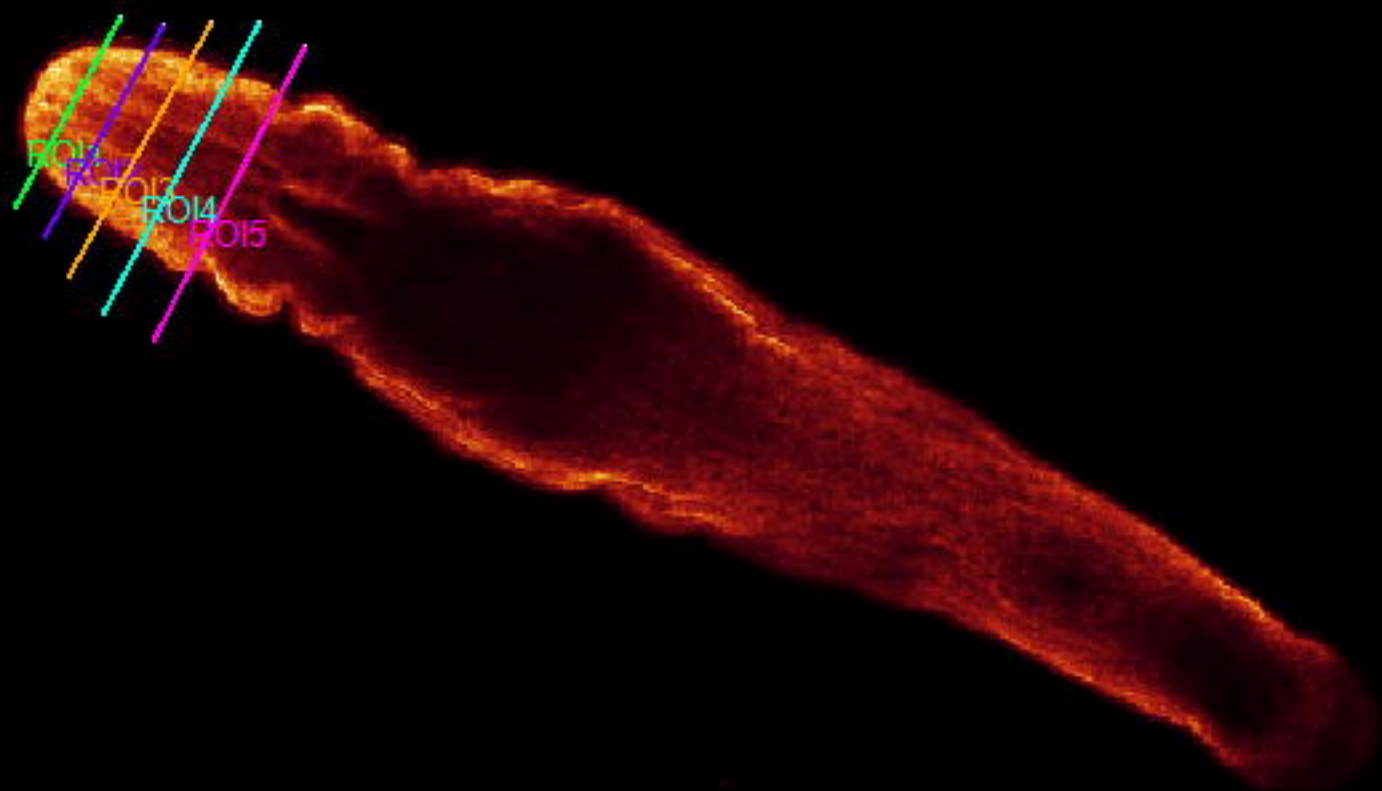
821 Fig. 2: Wide-field fluorescing imaging of *M. lignano* individuals stained with BCECF
822 under the four treatments considered in the study: a) anoxia followed by reoxygenation,
823 b) Near anoxia, c) Normoxia and d) Hyperoxia.

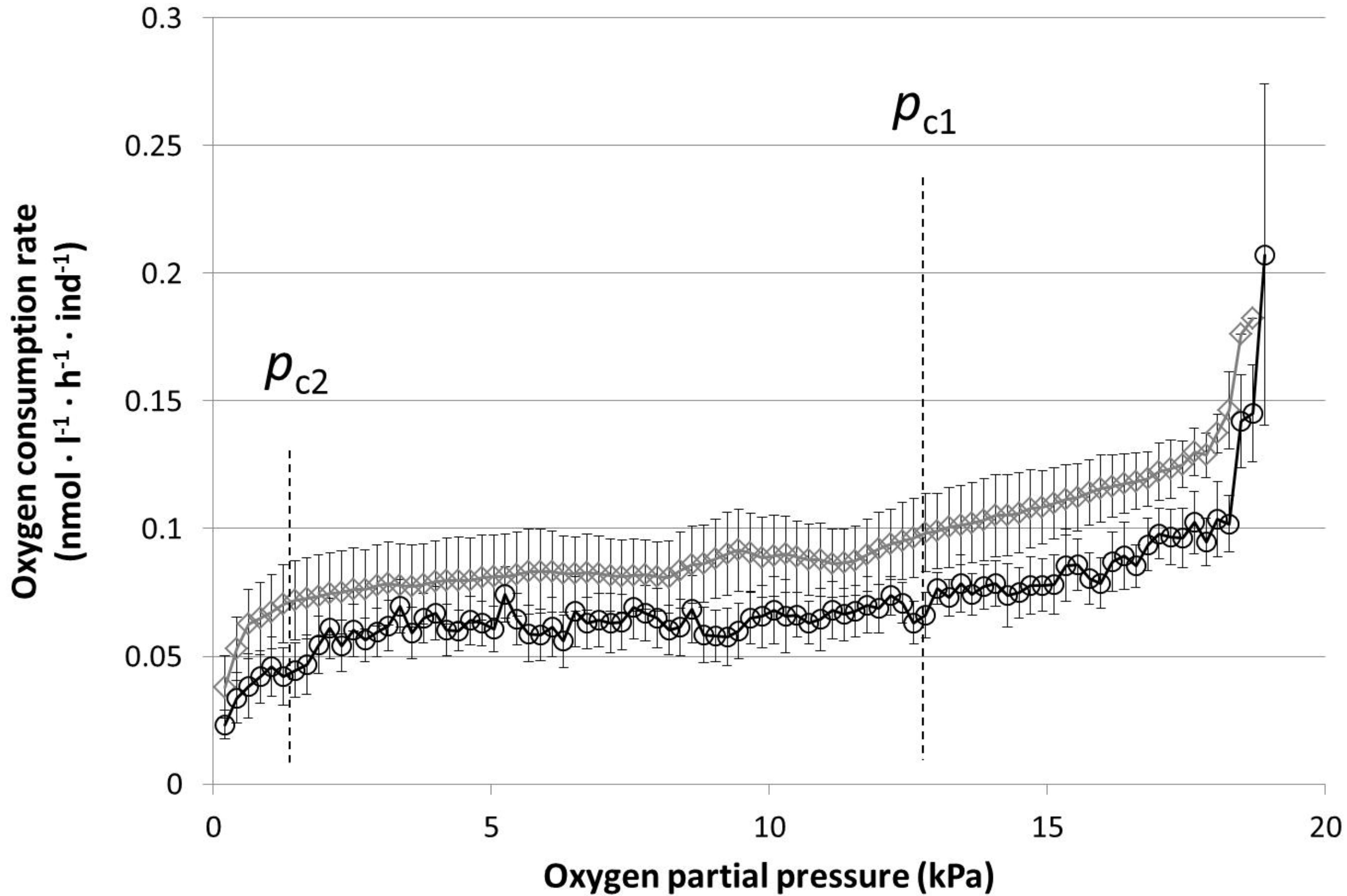
824

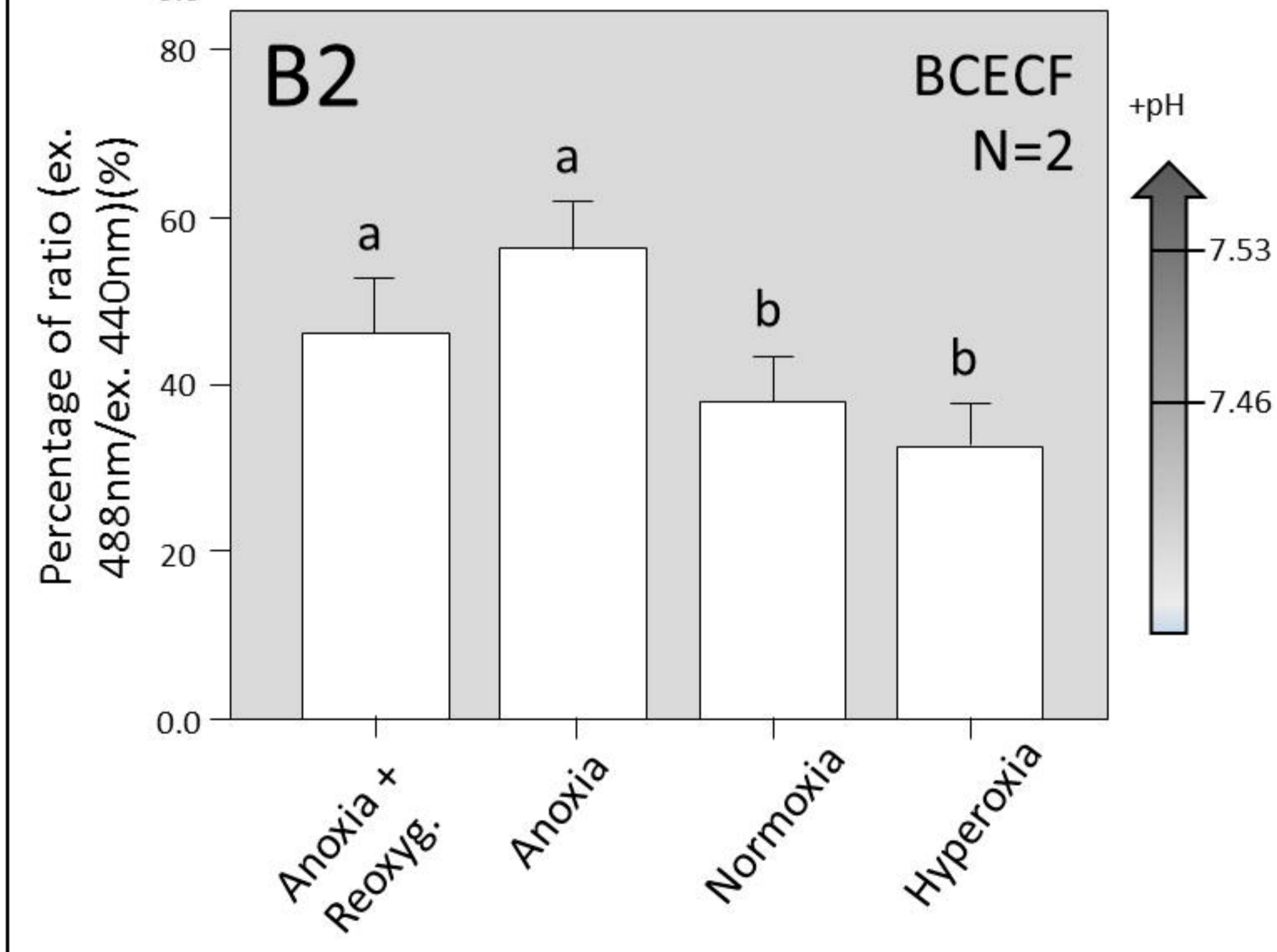
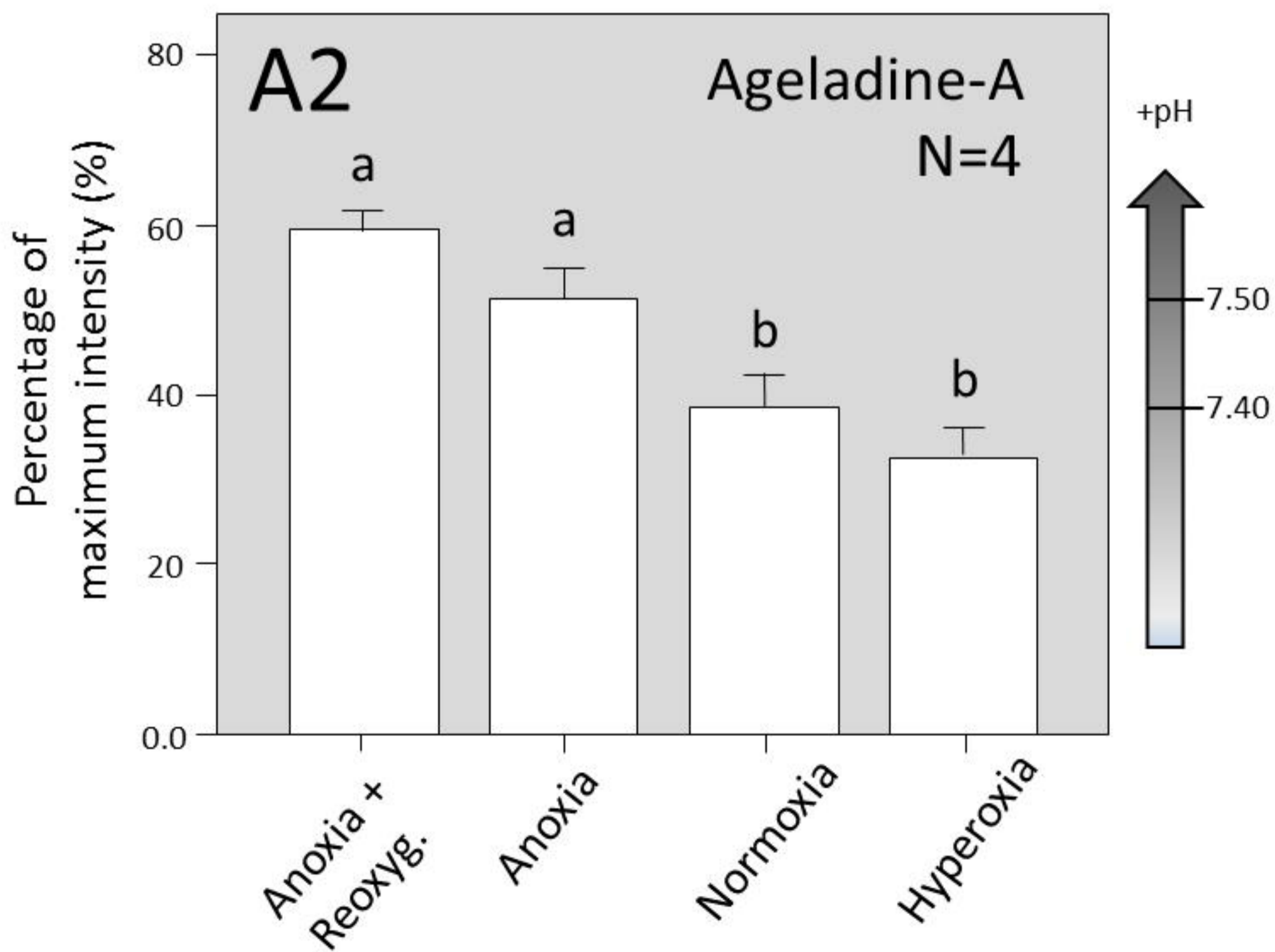
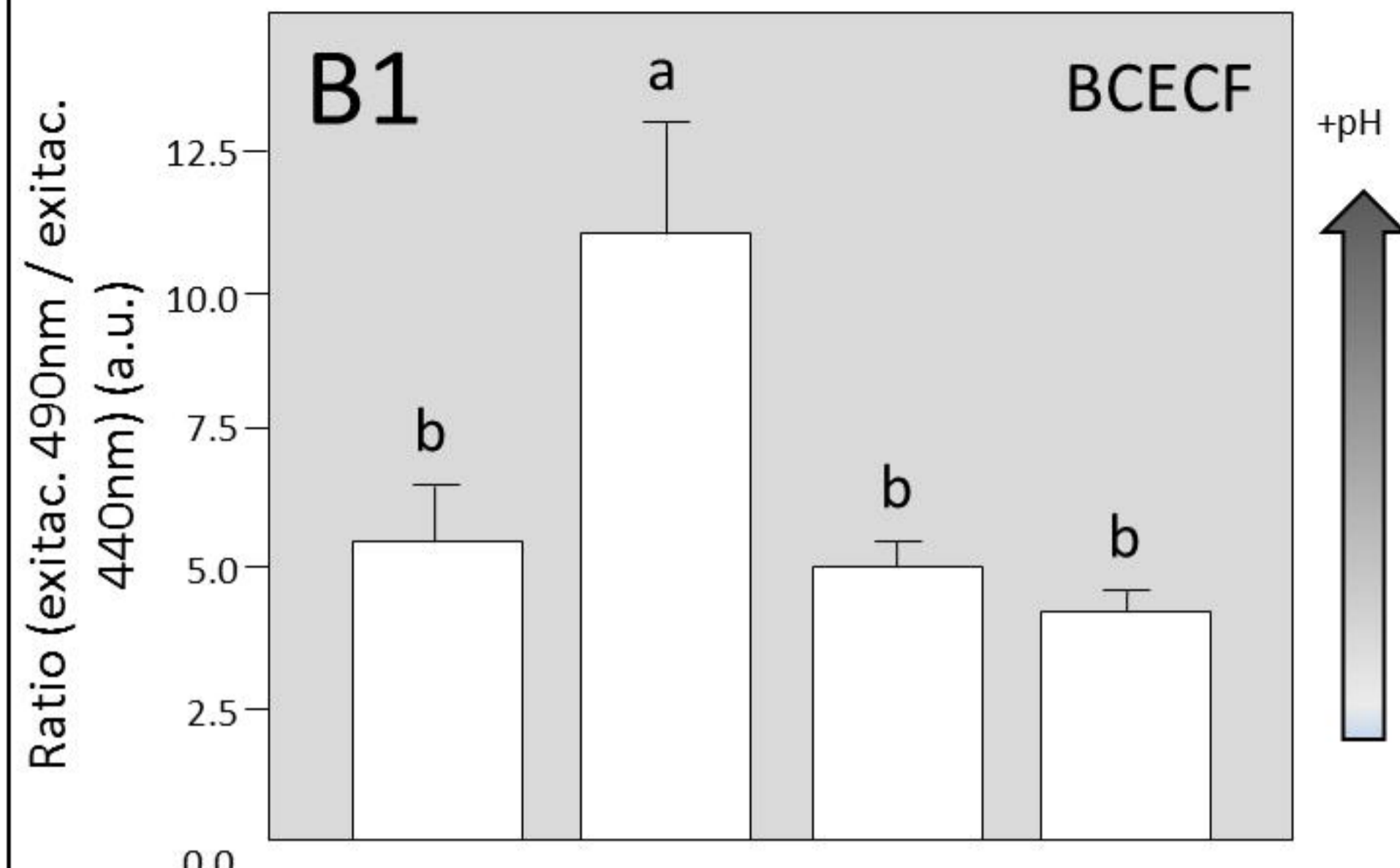
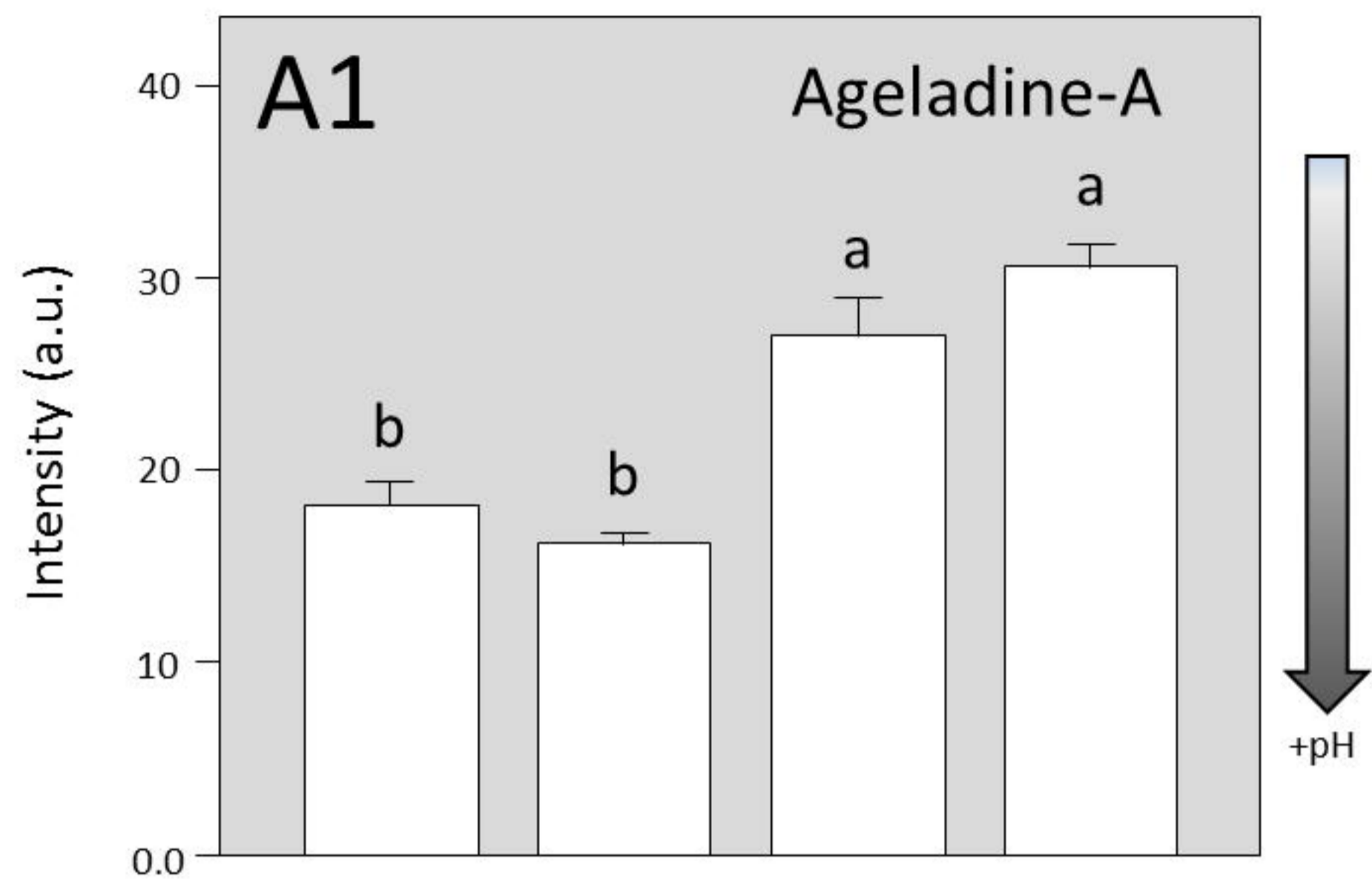
825 Fig. 3: Representative fluorescence images obtained during the mitochondrial
826 measurements under the confocal microscope for each of the treatments considered. Use
827 of A) MitoTracker Green Fm and (B) MitoTracker Deep Red 633 for mitochondrial
828 mass estimation and (C) JC-1 for $\Delta\psi_m$ calculation.

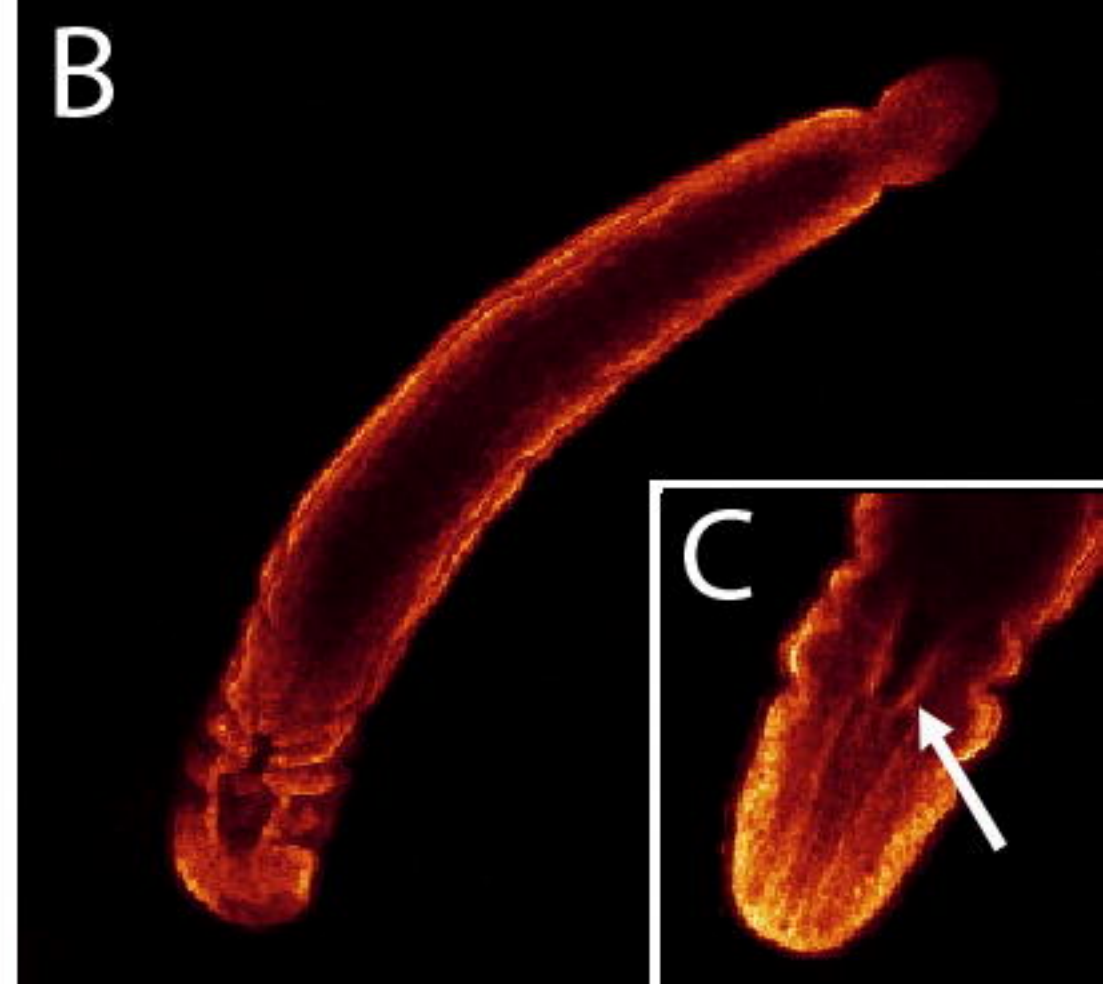
829

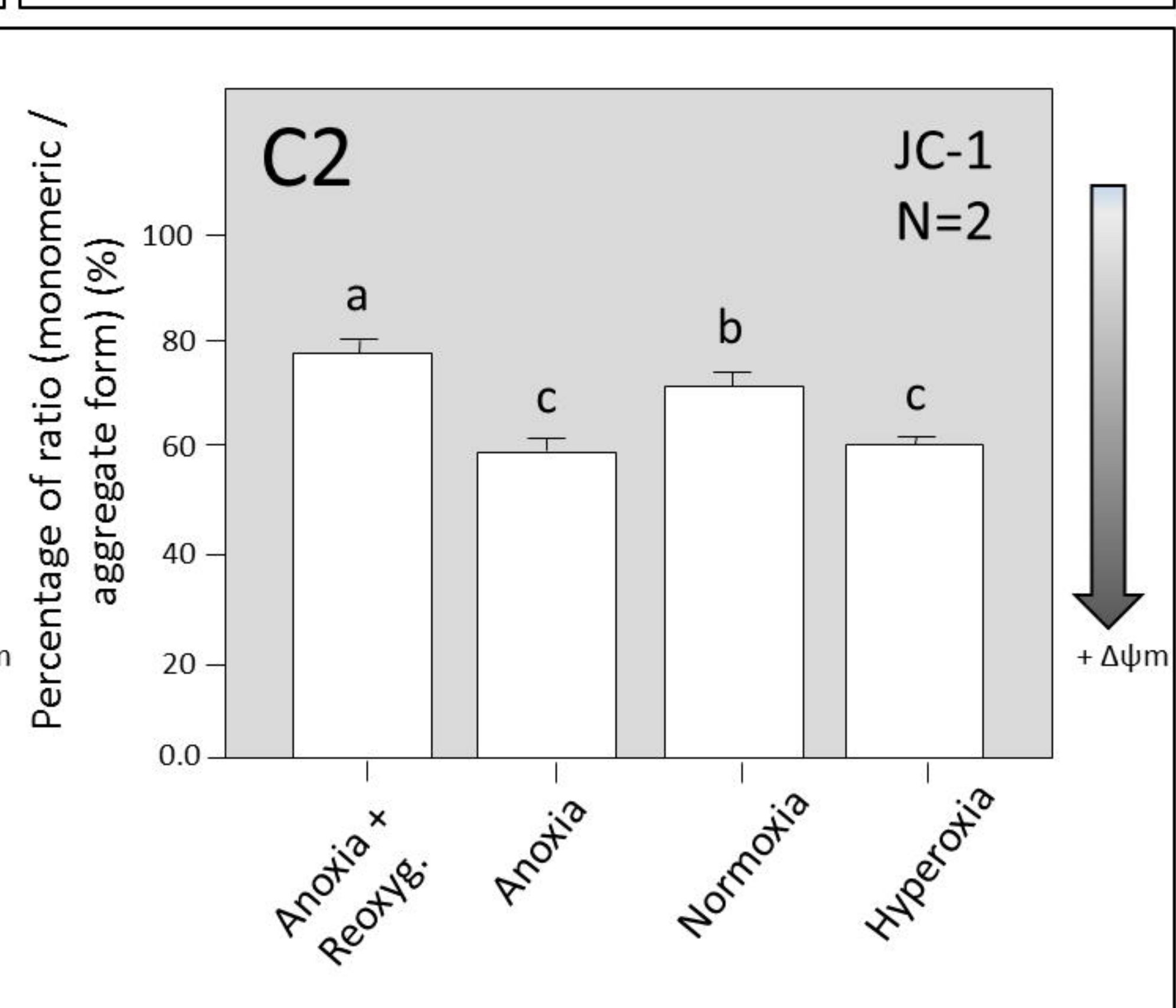
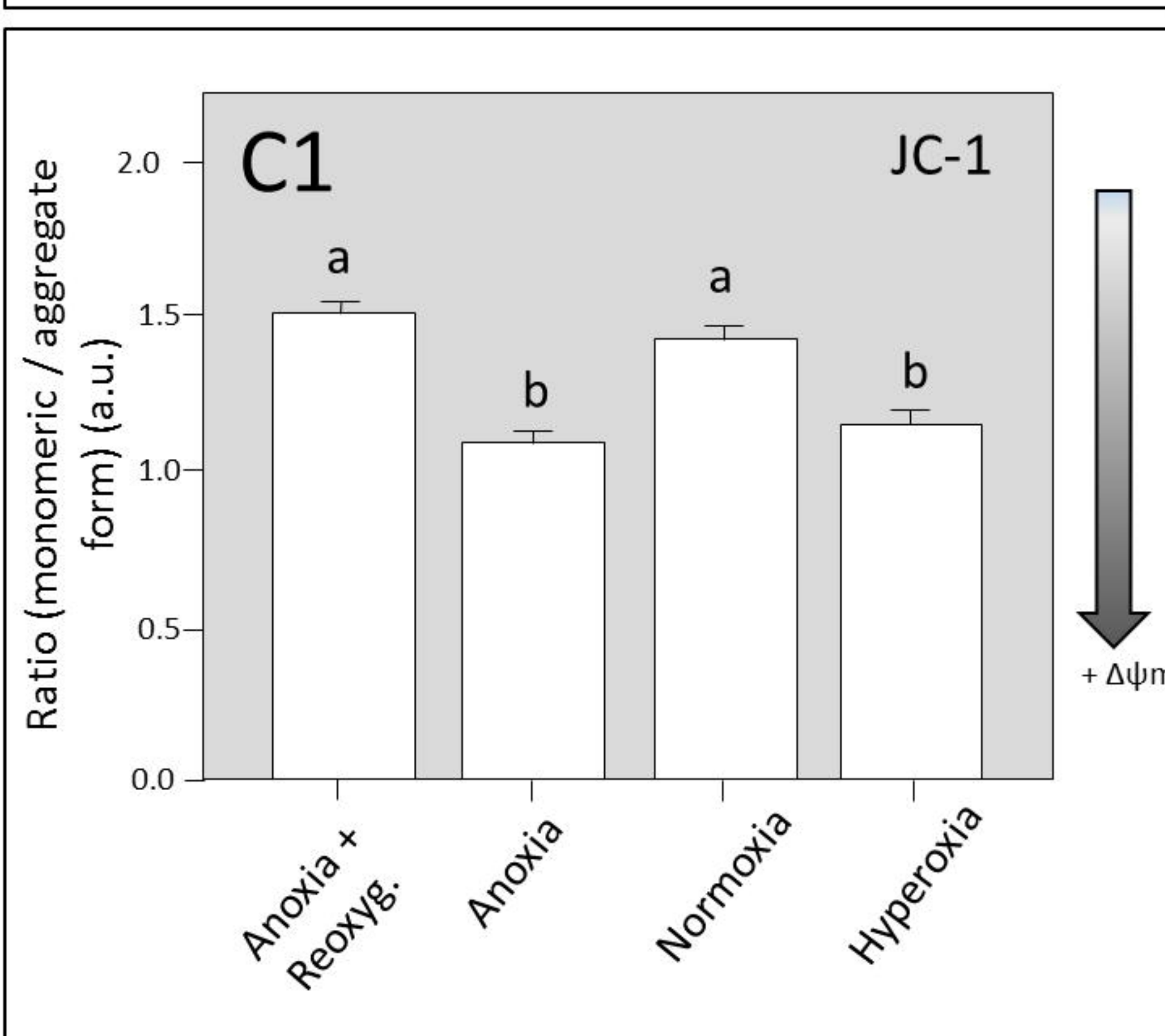
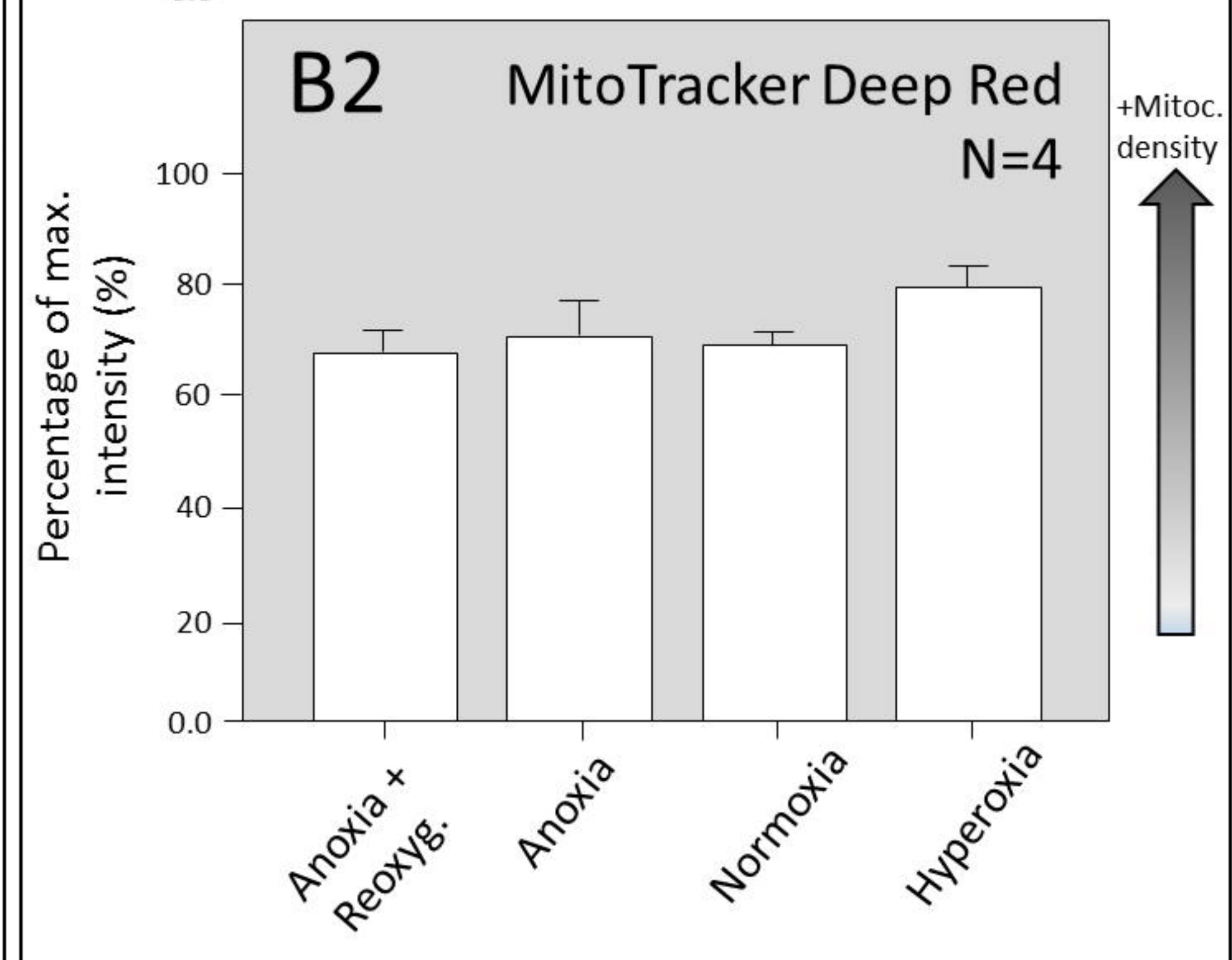
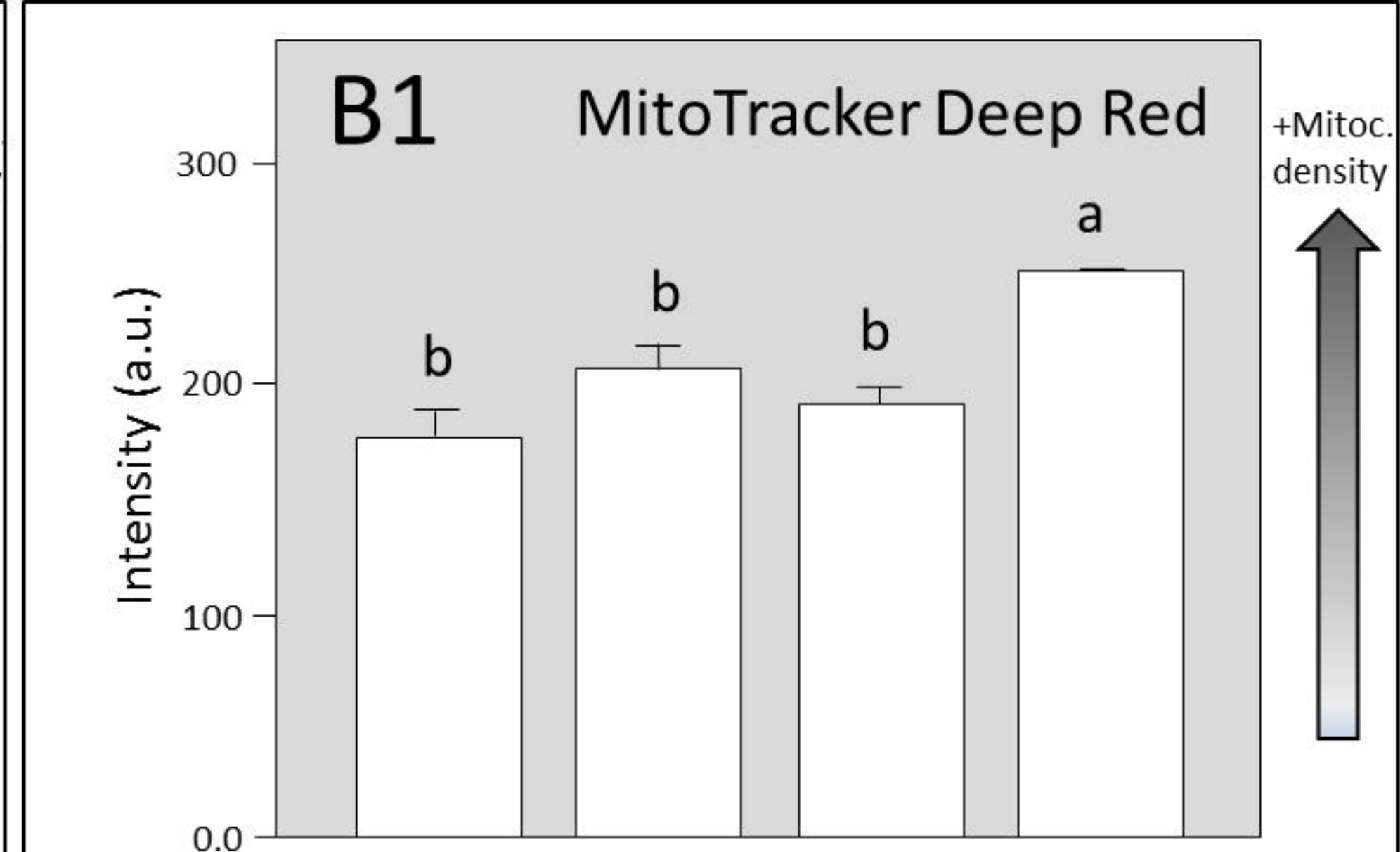
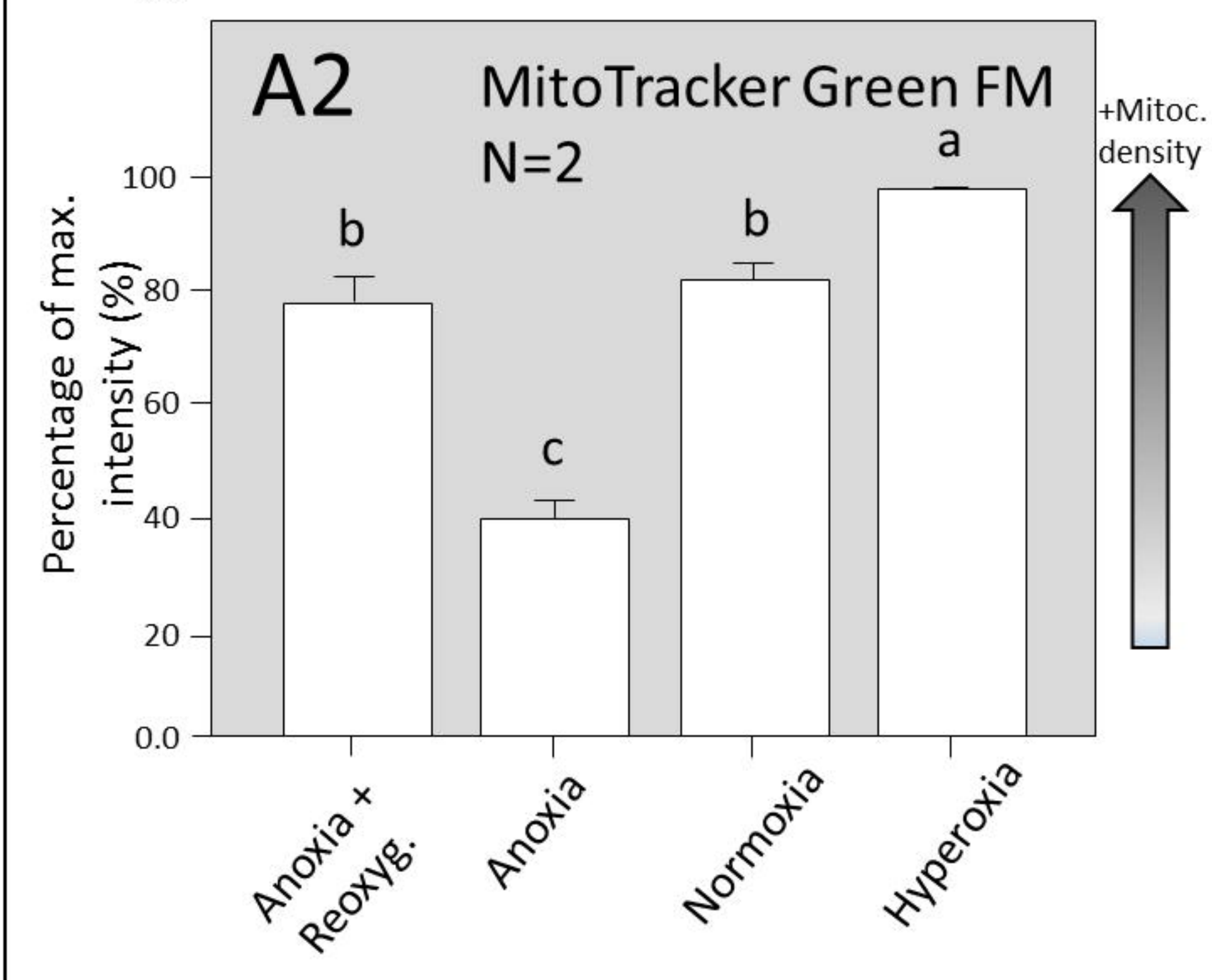
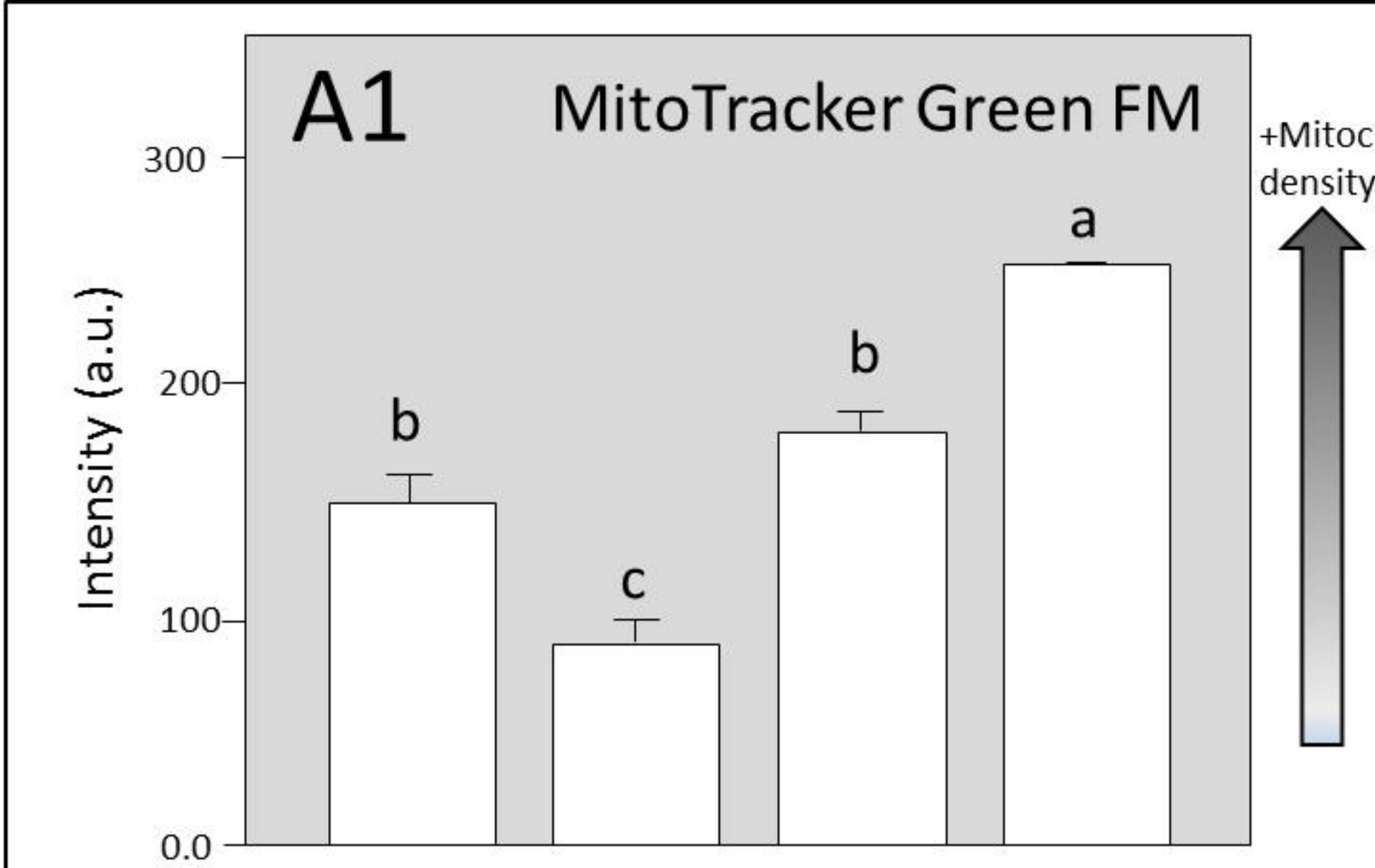
830 Fig. 4: Representative fluorescence images obtained during ROS quantification under
831 the confocal microscope for each of the treatments considered. Use of A) DHE and B)
832 C-H₂DFFDA for O₂• and H₂O₂ quantification, respectively.

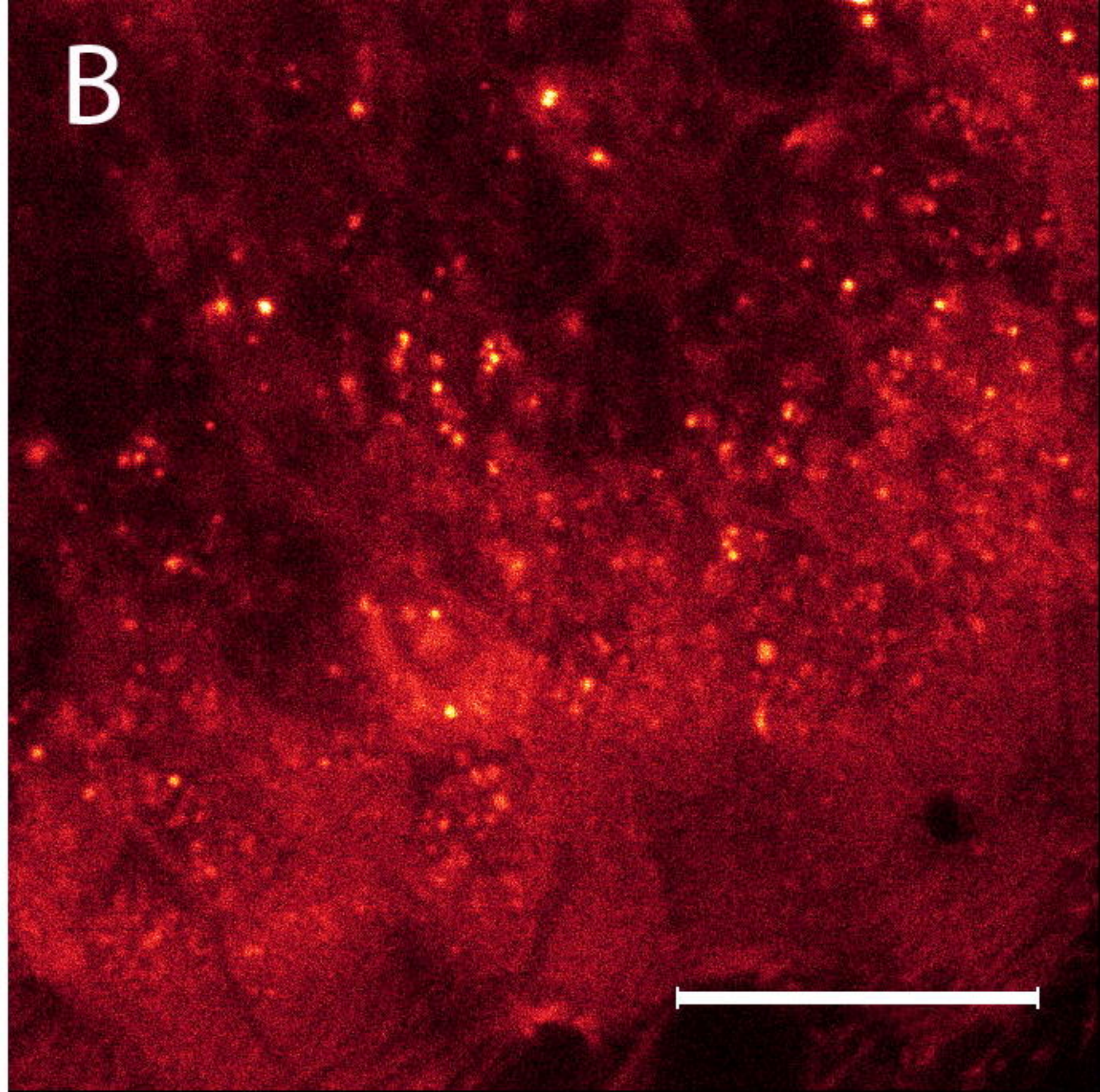
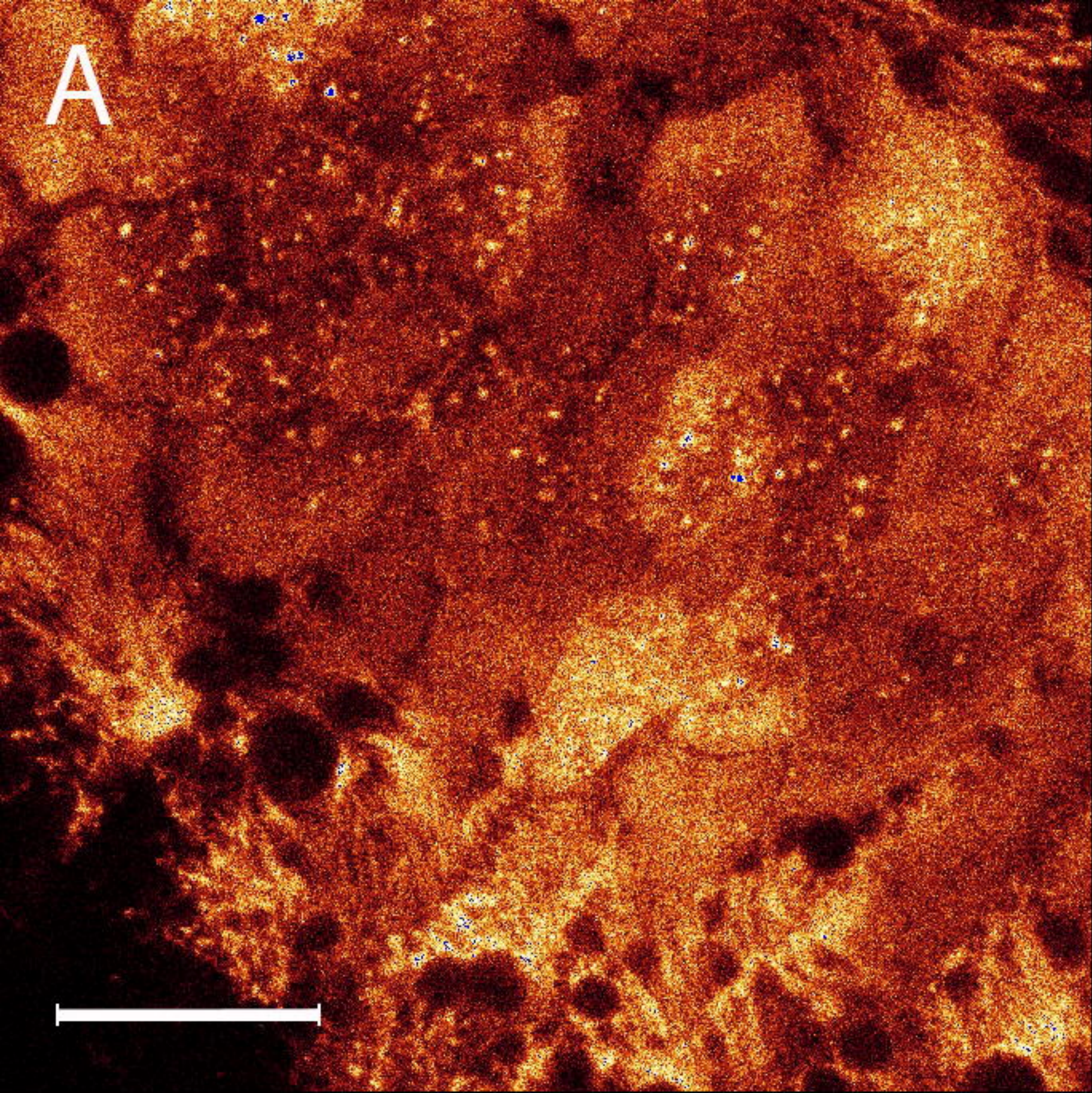
A**B**

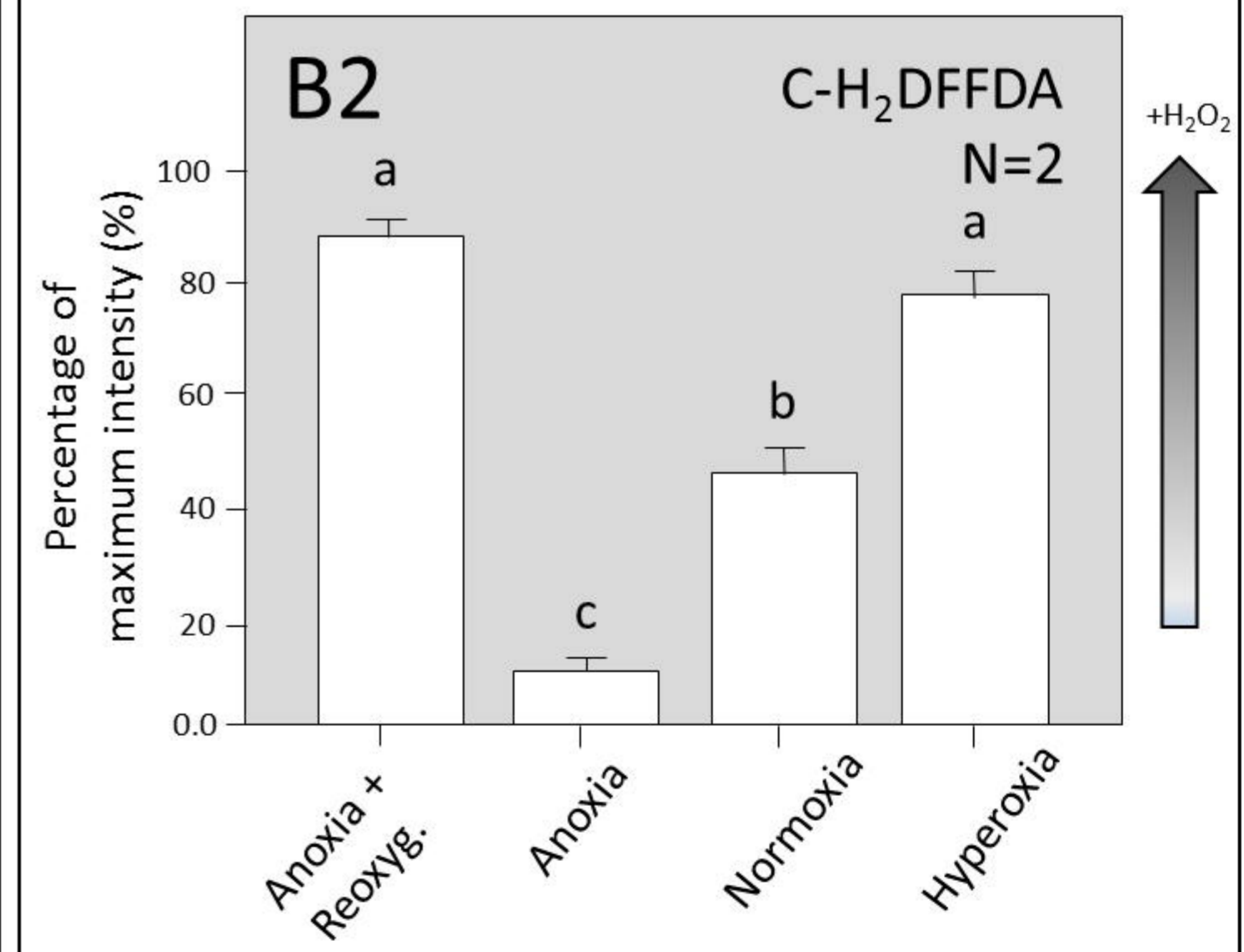
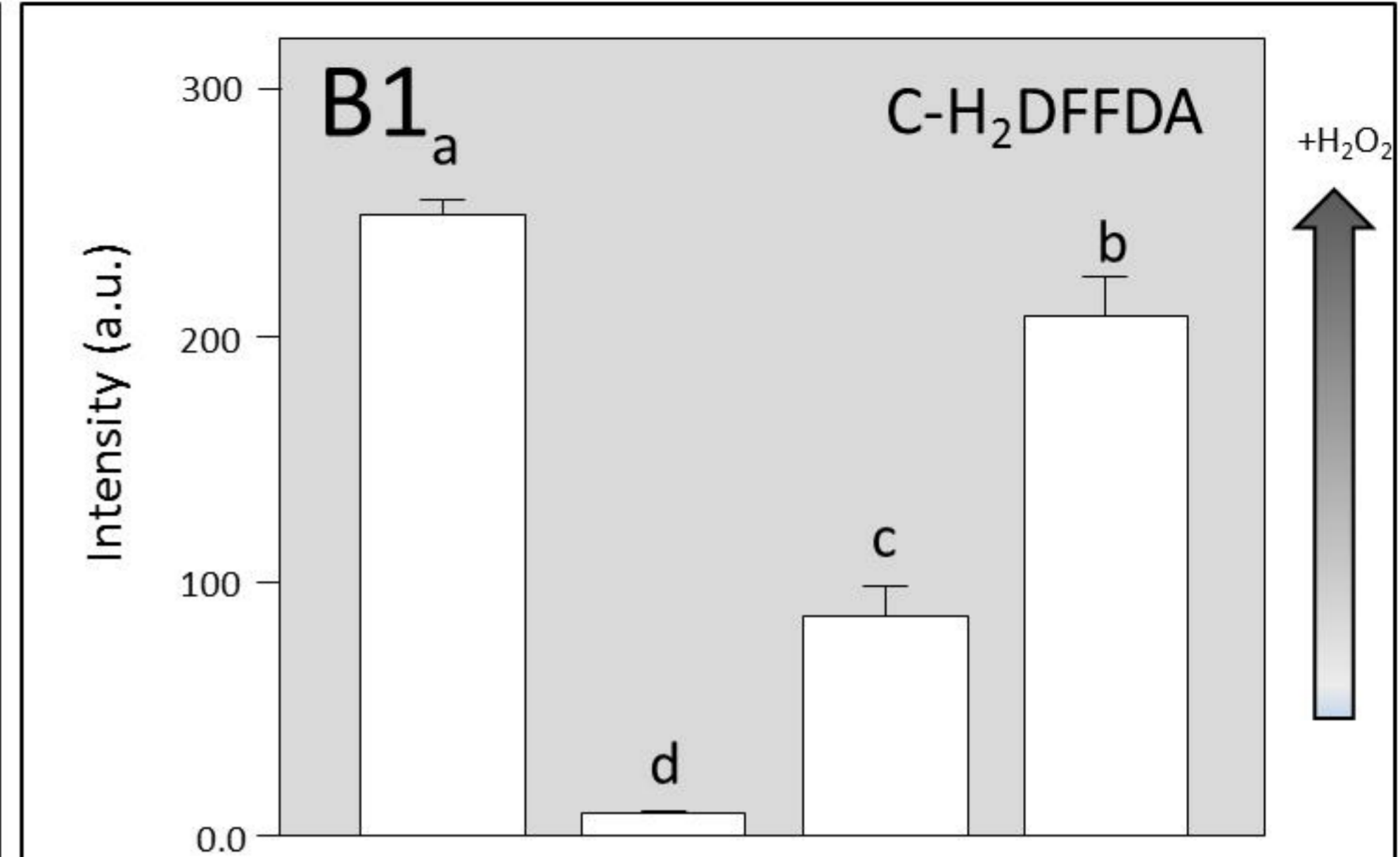
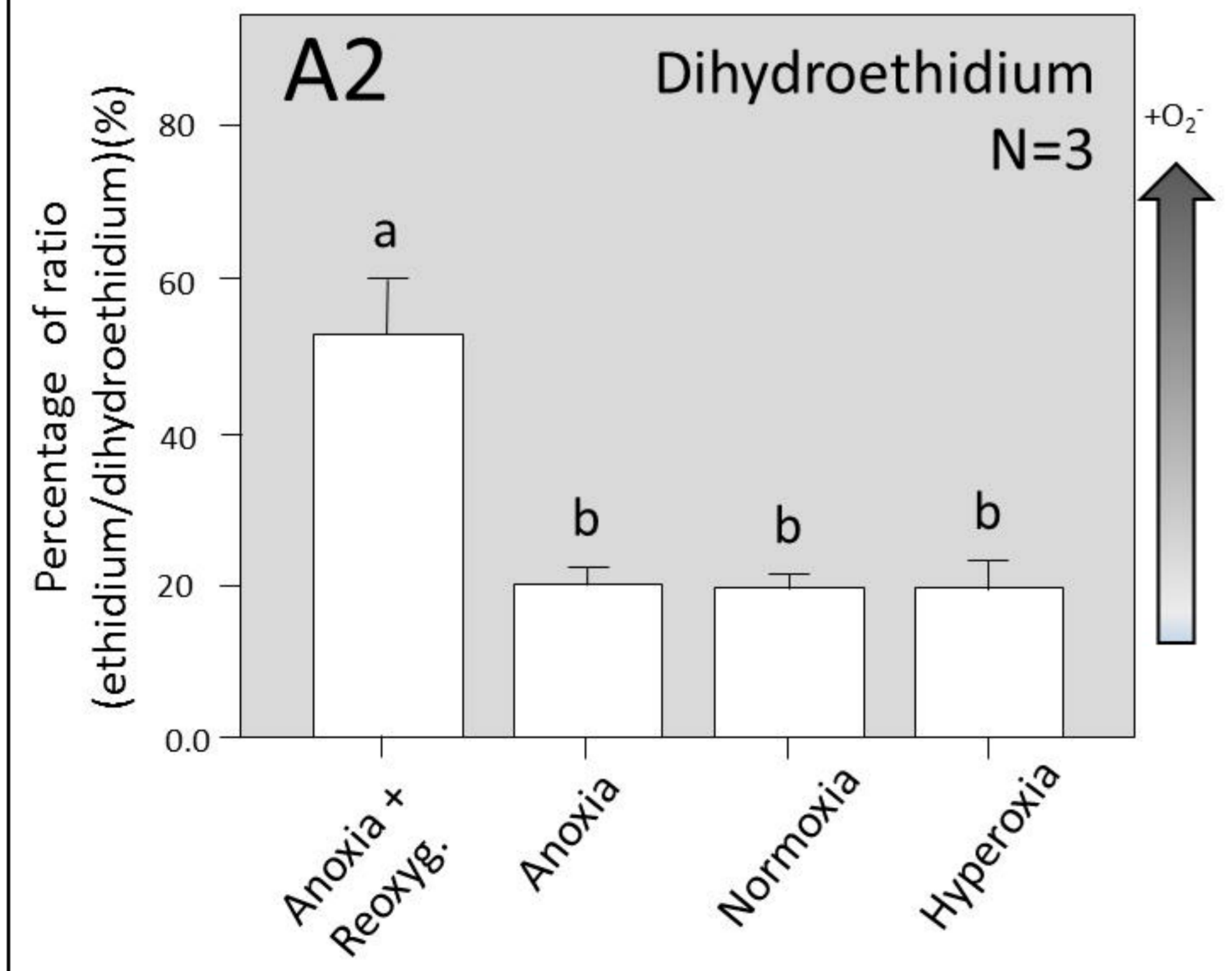
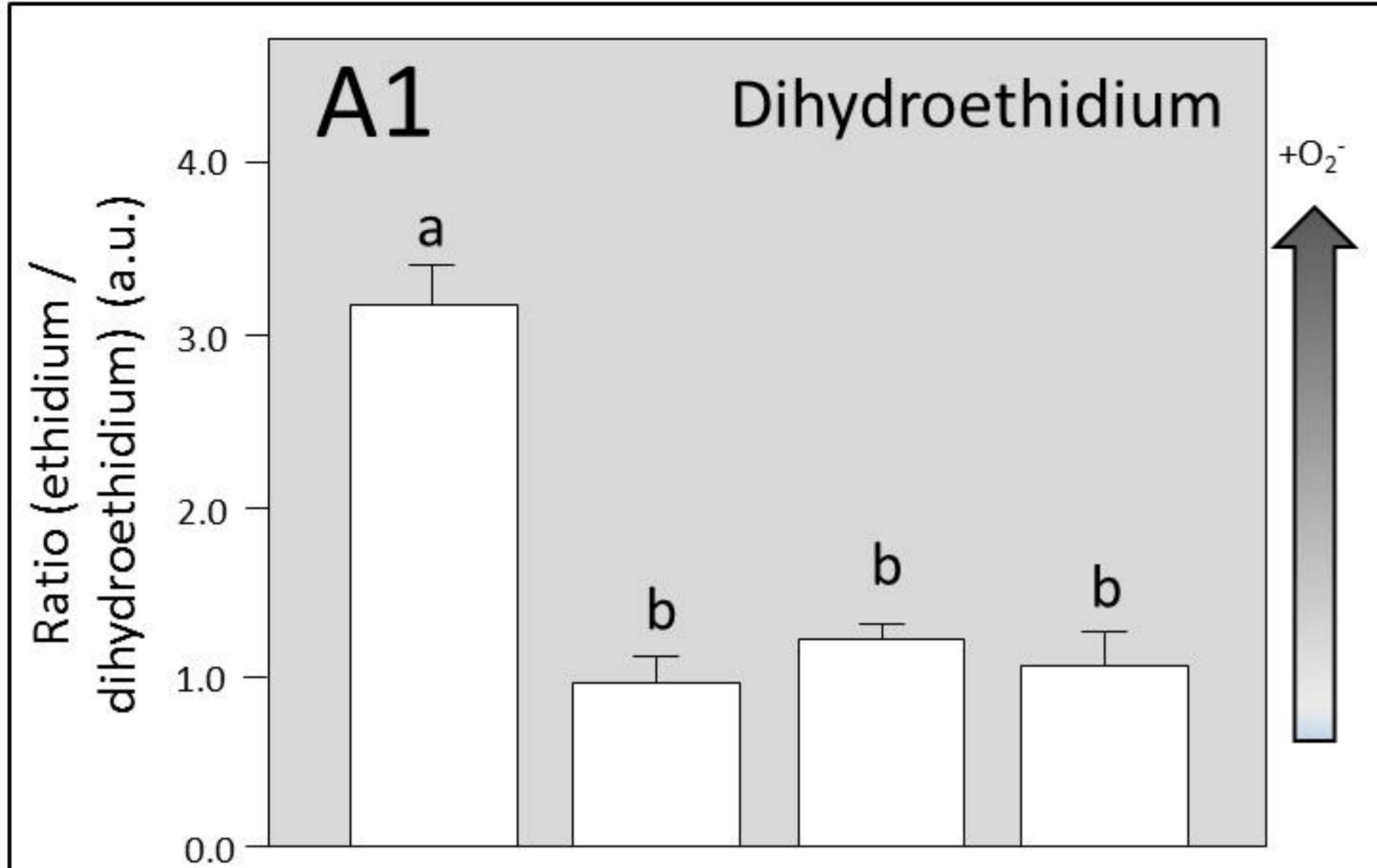












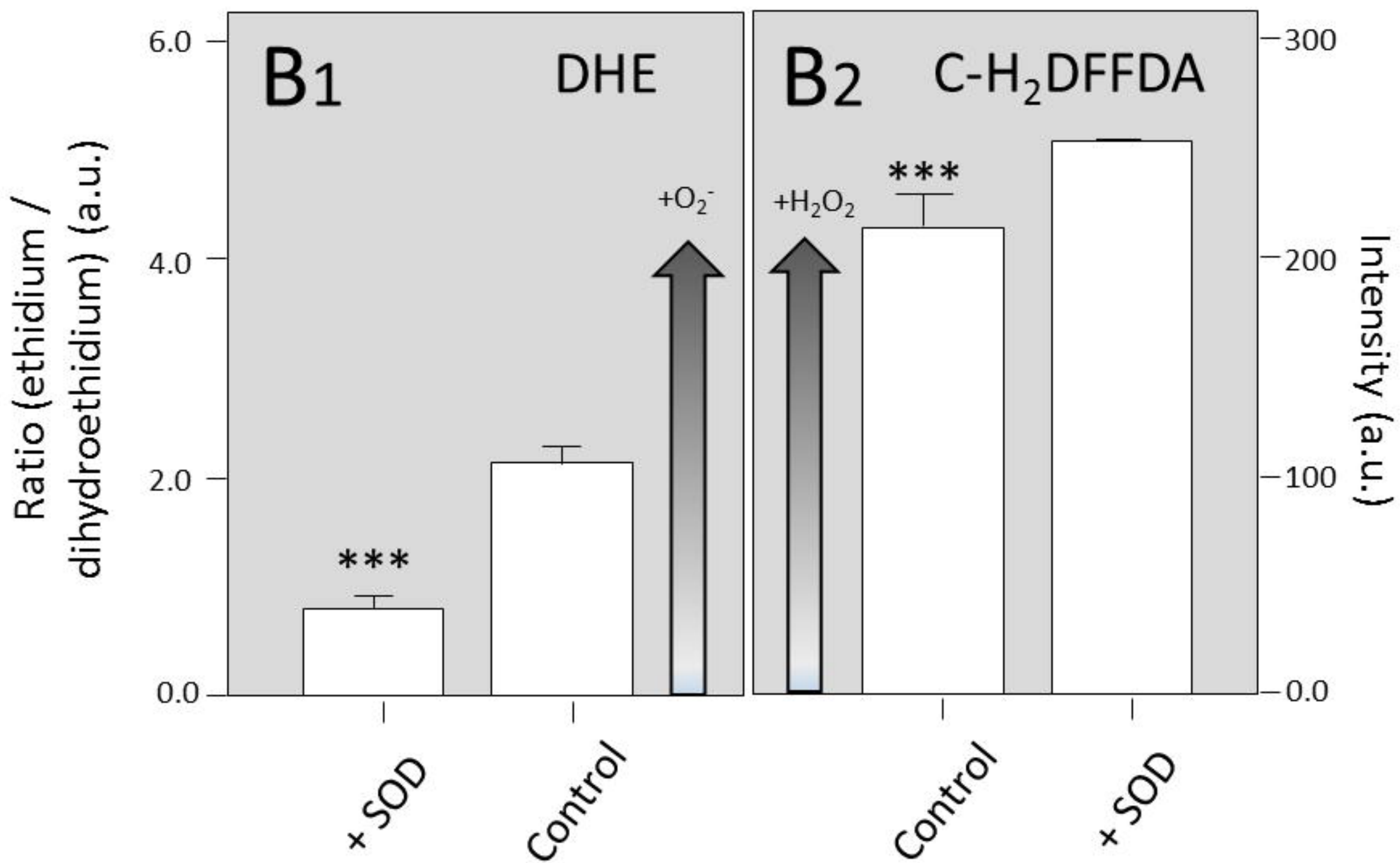
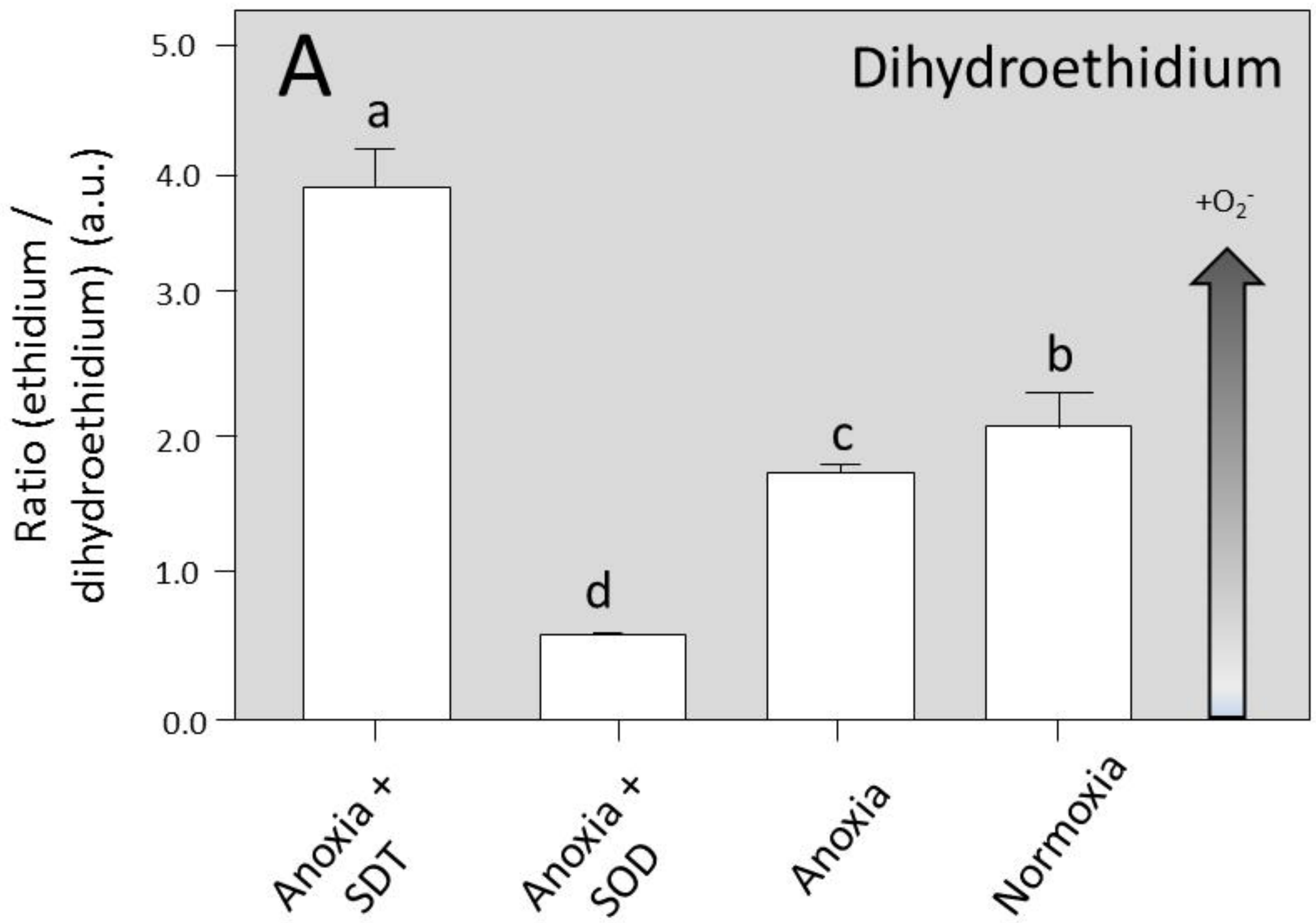


Table 1: Description of the dyes used during the present study:

Dye	Parameter measured	Company/code	Mechanism of function
Ageladine-A (in DMSO)	pH	**	Probe which exists as a nearly uncharged monomer under pH of 8.1-8.6. After crossing cellular membranes, becomes charged in the cytosol and acidic compartments of cells.
BCECF AM (in DMSO)	pH	Molecular Probes (B-3051)	Probe which absorption shifts whether it occurs as the basic (phenolate anion) or acidic (protonated) form.
MitoTracker Green FM (in DMSO)	Mitochondrial density	Molecular Probes (M-7514)	Non-fluorescent molecule which becomes fluorescent once accumulates in the lipid environment of the mitochondria.
MitoTracker Deep Red 633 (in DMSO)	Mitochondrial density	Molecular Probes (M-22426)	Non-fluorescent molecule which becomes fluorescent once accumulates in the lipid environment of the mitochondria.
JC-1 (in DMSO)	Mitochondrial membrane potential	Molecular Probes (T-3168)	This green fluorescent probe exists as a monomer at low $\Delta\psi_m$. With high $\Delta\psi_m$ values, JC-1 aggregates and shows a red fluorescence.
Dihydroethidium (DHE) (in DMSO)	$O_2^{\bullet-}$	Molecular Probes (D-23107)	Regularly shows a blue emission when excited with a 355nm laser. When oxidized by the presence of $O_2^{\bullet-}$, it intercalated with the DNA and shows a red emission when excited with an argon laser.
C-H ₂ DFFDA (in Ethanol)	H ₂ O ₂ , HOO• and ONOO ⁻	Molecular Probes (C-13293)	Non-fluorescent molecule which is converted to a green-fluorescent form when the acetate groups are removed by intracellular esterases and oxidation occurs in the cell.

** Synthesized by Peter Karuso, Macquarie University, Sydney.

Table 2: Analysis conditions for each of the dyes used during the study.

Dye	Final conc. used (μM)	Incubation time (min)	N ind per batch	N repetitions (total N individuals)	Excitation		Emission		Calculation
					λ_1 (nm)	λ_2 (nm)	PMT1 (nm)	PMT2 (nm)	
Ageladine-A (in DMSO)	15	90	10	4 (50)	MP(370)	-	420-500	-	Maximum Intensity
BCECF AM (in DMSO)	5.0	90	10	2 (20)	MP(439)	488	520-550	-	Maximum values ratio λ_2/λ_1
MitoTracker Green FM (in DMSO)	0.33	30	10	2 (20)	488	-	500-550	-	Maximum intensity
MitoTracker Deep Red 633 (in DMSO)	0.33	60	10	4 (40)	633	-	640-680	-	Maximum intensity
JC-1 (in DMSO)	5	60	10	2 (20)	488	488	500-550	560-600	Ratio PMT1/PMT2
Dihydroethidium (DHE) (in DMSO)	3.3	30	10	3 (30)	MP (355)	488	400-440	620-660	Ratio PMT2/PMT1
C-H ₂ DFFDA (in Ethanol)	10.6	30	10	2 (20)	488	-	510-550	-	Maximum Intensity

MP=Multiphoton laser. Values in parenthesis indicate the effective excitation wavelength.